Activation of Nedd4L Ubiquitin Ligase by FCHO2-generated Membrane Curvature

Yasuhisa Sakamoto[1], Akiyoshi Uezu[1,2], Koji Kikuchi[1], Shiro Suetsugu[3], and Hiroyuki Nakanishi[1,*]

[1]Department of Molecular Pharmacology, Faculty of Life Sciences, Kumamoto University, 1-1-1 Honjyo, Kumamoto 860-8556, Japan

[2]Present address, Department of Cell Biology, Duke University Medical School, Durham, North Carolina 27710, U.S.A

[3]Division of Biological Science, Graduate School of Science and Technology, Nara Institute of Science and Technology, Ikoma 630-0192, Japan

[*]Corresponding author. Tel: +81-96-373-5074; Fax: +81-96-373-5078; E-mail: hnakanis@gpo.kumamoto-u.ac.jp

Summary

The C2-WW-HECT domain ubiquitin ligase Nedd4L regulates sorting in endocytosis by mediating ubiquitination of cargo molecules, such as the epithelial sodium channel (ENaC)[1,2]. Defects in ENaC ubiquitination cause Liddle syndrome, a hereditary hypertension. Nedd4L is catalytically autoinhibited by an intramolecular interaction between the C2 and HECT domains[3], but the activation mechanism is poorly understood. Here, we show that Nedd4L is activated by membranes sculpted by FCHO2, a Bin-Amphiphysin-Rsv (BAR) domain protein that regulates endocytosis. We found that

FCHO2 was required for Nedd4L-mediated ubiquitination and endocytosis of ENaC. Nedd4L co-localized with FCHO2 at clathrin-coated pits where it likely became activated. Nedd4L was specifically recruited to and activated by the FCHO2 BAR domain exogenously expressed in cells. Furthermore, we reconstituted *in vitro* FCHO2-induced recruitment and activation of Nedd4L. Both the recruitment and activation were mediated by membrane curvature rather than protein–protein interactions. The Nedd4L C2 domain recognized a specific degree of membrane curvature that was generated by the FCHO2 BAR domain. Consequently, this curvature activated Nedd4L by relieving autoinhibition. Thus, we show for the first time a specific functionality (i.e., recruitment and activation of an enzyme regulating cargo sorting) of membrane curvature by a BAR domain protein.

Main

Nedd4L is a member of the Nedd4 family of HECT-type E3 ubiquitin (Ub) ligases, which are characterized by a common modular organization, with an N-terminal C2 domain, two to four WW domains, and a C-terminal catalytic HECT domain. At least some of the family members, including Nedd4L, are catalytically autoinhibited by an intramolecular interaction between the C2 and HECT domains[3,4]. However, the activation mechanism of the Nedd4 family is poorly understood. Nedd4L regulates the trafficking of membrane receptors, transporters, and ion channels, such as the epithelial sodium channel (ENaC). This channel is composed of three subunits, α, β, and γENaC[2]. Nedd4L specifically mediates ENaC ubiquitination at the plasma membrane. Ubiquitinated ENaC is recognized by adaptor proteins for clathrin-mediated endocytosis (CME) and is consequently internalized.

FCHO2 is required for ubiquitination and endocytosis of ENaC

Membrane-sculpting Bin-Amphiphysin-Rsv (BAR) domain proteins play crucial roles in CME[5–7]. BAR domains form a crescent-shaped dimer characterized by a specific degree of intrinsic curvature. They bind to negatively-charged phospholipids, such as phosphatidylserine (PS), and force membranes to bend according to their intrinsic curvatures, thereby inducing the formation of membrane tubules with specific diameters (curvatures). For example, the diameters of membrane tubules generated by the amphiphysin BAR domain, FCHO2 BAR domain, and FBP17 BAR domain are 20–50 nm (sharper curvature)[8–10], 50–80 nm (intermediate curvature)[11], and ~150 nm[12] (shallower curvature), respectively. The BAR domain protein FCHO2 is proposed to initiate the formation of clathrin-coated pits (CCPs)[5,13]. FCHO2 binds to the flat surface of the plasma membrane at sites where CCPs will form. FCHO2 then generates the initial membrane curvature and recruits the clathrin machinery for CCP formation.

We first examined the role of FCHO2 in Nedd4L-mediated ubiquitination and endocytosis of ENaC using a HeLa cell line stably expressing all three subunits, α, β, and γENaC (αβγENaC-HeLa cells) (Extended Data Fig. 1a-c). Upon FCHO2 knockdown by small interfering RNA (siRNA) methods, ENaC internalization was reduced, as was upon Nedd4L knockdown[14] (Fig. 1a, and Extended Data Fig. 2a). This phenotype was rescued by an siRNA-resistant (sr) form of FCHO2 (Extended Data Fig. 2b). Furthermore, FCHO2 or Nedd4L knockdown reduced αENaC ubiquitination at the cell surface (Fig. 1b). These results suggest that FCHO2 is required for Nedd4L-mediated ubiquitination and endocytosis of ENaC.

Recruitment and activation of Nedd4L by FCHO2 in cells

Immunofluorescence microscopy revealed that in αβγENaC-HeLa cells, cell-surface αENaC co-localized with FCHO2 at CCPs (Fig. 1c). However, its co-localization with Nedd4L was not detected (Extended Data Fig. 2c), because exogenous expression of Nedd4L stimulated ENaC internalization, resulting in the disappearance of αENaC from the cell surface. In wild-type HeLa cells, Nedd4L accumulated at CCPs where FCHO2 localized (Fig. 1d). The co-localization of FCHO2 and Nedd4L at CCPs prompted us to investigate whether they interact with each other.

Expression of Nedd4L exhibited diffuse distribution throughout the cytoplasm in COS7 cells (Fig. 2a). However, co-expression of the FCHO2 BAR domain [amino acid (aa) 1-302] recruited Nedd4L to membrane tubules. The Nedd4L C2 domain (Myc-Nedd4L C2, aa 1-160) was also concentrated to membrane tubules, whereas C2 domain-deleted Nedd4L (Myc-Nedd4L ΔC2) was not. In contrast to FCHO2, the FBP17 BAR domain did not recruit Nedd4L to membrane tubules. Additionally, the BAR domain protein amphiphysin1 did not recruit Nedd4L to membrane tubules. Thus, Nedd4L is selectively recruited through the C2 domain to membrane tubules generated by the FCHO2 BAR domain. Similar results were obtained in HEK293 cells (Extended Data Fig. 3a).

We also investigated whether FCHO2 not only recruits but also activates Nedd4L in cells. For this purpose, we performed an *in vivo* ubiquitination assay using HEK293 cells. As the catalytic activity of E3 Ub ligases is typically reflected in their autoubiquitination[4], we determined activity by measuring the ubiquitination level of

Nedd4L itself. Expression of the FCHO2 BAR domain in cells remarkably enhanced Nedd4L autoubiquitination, whereas FBP17 or amphiphysin1 did not (Fig. 2b). Tubulation-deficient FCHO2 mutants (K146E+R152E and L136E)[5] did not enhance Nedd4L activity (Fig. 2b, c, Extended Data Fig. 3b, and Extended Data Fig. 4). A catalytically inactive Nedd4L mutant, C922A, which was recruited to FCHO2-generated membrane tubules, showed little enhancement of ubiquitination upon FCHO2 expression (Fig. 2d, and Extended Data Fig. 3c), indicating that Nedd4L ubiquitination is self-induced. Using αENaC as a substrate, we further confirmed that Nedd4L is activated upon FCHO2 expression in cells (Extended Data Fig. 5). Thus, Nedd4L is specifically recruited to and activated by membrane tubules generated by FCHO2 in cells.

Preference of Nedd4L for FCHO2-generated membrane curvature

The aforementioned results prompted us to investigate whether FCHO2 and Nedd4L interact through membrane tubules rather than through stereotyped protein–protein interactions. Membrane tubules generated by BAR domains in cells have specific diameters (curvatures) as described above. Nedd4L may preferentially bind to the specific degree of membrane curvature generated by FCHO2. To investigate this possibility, we first examined the biochemical properties of Nedd4L. Using a co-sedimentation assay with Folch liposomes made of PS-rich (~50%) bovine lipids (Folch fraction 1) and synthetic liposomes containing various percentages of PS, we found that the C2 domain of Nedd4L is a Ca^{2+}-dependent PS-binding domain (Extended Data Fig. 6a, b). Submicromolar Ca^{2+} concentrations, which are comparable to intracellular levels in unstimulated cells, were sufficient for the Nedd4L C2 domain to bind to PS-containing

liposomes. The C2 domain alone and full-length Nedd4L showed different Ca^{2+} requirements. The higher Ca^{2+} requirement of full-length Nedd4L may be due to the intramolecular interaction between the C2 and HECT domains. Increasing PS percentages in synthetic liposomes enhanced the liposome binding of the Nedd4L C2 domain, and PS requirements varied depending on Ca^{2+} concentration.

We next examined whether Nedd4L preferentially binds to a specific degree of membrane curvature. For this purpose, liposomes of different sizes (curvatures) were prepared by stepwise extrusion through filter membranes with different pore sizes (0.8, 0.4, 0.2, 0.1, 0.05, and 0.03 μm) and sonication (Extended Data Fig. 7). Sonication or extrusion through a 0.03 μm pore-size filter was used to prepare the smallest liposomes. Transmission electron microscopy revealed that the actual liposome size was similar to the pore size for 0.2, 0.1, 0.05, and 0.03 μm pore-size liposomes, whereas it was significantly smaller for 0.8 and 0.4 μm pore-size liposomes. Nedd4L showed the strongest binding to 0.05 μm pore-size liposomes (Fig. 3a).

Synaptotagmin I (SytI) tandem C2 domains can both generate and sense membrane curvature *in vitro* by penetrating their hydrophobic residues into the lipid bilayer[15]. As a sensor, the binding affinity is considered to be highest for membranes that have a degree of curvature consistent with that generated by SytI itself. We investigated whether, in addition to sensing membrane curvature, the Nedd4L C2 domain can also generate membrane curvature *in vitro* and, if so, what diameter of membrane tubules is generated. As expected, transmission electron microscopy revealed that the C2 domain deformed liposomes into extensive tubulation (Fig 3b). The tubule diameter was mainly 40–80 nm, which is consistent not only with the diameter of 0.05 μm pore-size liposomes,

to which Nedd4L preferentially binds, but also with the diameter of membrane tubules generated by FCHO2 (Fig. 3c and see Extended Data Fig. 7). These results suggest that Nedd4L shows the highest binding affinity for the degree of membrane curvature generated by FCHO2. It is therefore likely that FCHO2-induced recruitment and activation of Nedd4L are mediated by the degree of membrane curvature.

Roles of conserved hydrophobic residues in the Nedd4L C2 domain

We compared the C2 domain sequence of Nedd4L to those of other Nedd4 family members, SytI, and protein kinase Cγ (PKCγ) (Extended Data Fig. 8a). SytI C2 domains possess hydrophobic residues (M173, F234, V304, and I367) for penetration into the lipid bilayer to generate and sense membrane curvature[15]. The Nedd4L C2 domain also has three hydrophobic residues (I37, F38, and L99), which are conserved among Nedd4 family members except for WWP2. We mutated these residues to alanine to produce six mutants, I37A, F38A, L99A, I37A+F38A, I37A+L99A, and I37A+F38A+L99A (triple-A). Any single mutation did not inhibit Nedd4L recruitment to FCHO2-generated membrane tubules (Extended Data Fig. 8b). However, double and triple mutations severely impaired this recruitment. Furthermore, the I37A+F38A and triple-A mutants showed little liposome binding and lost curvature generation (Fig. 3d, e). Thus, these hydrophobic residues (I37, F38, and L99) are critical for both membrane binding and curvature sensing and generation. These residues are likely inserted into the lipid bilayer, thereby strengthening the C2 domain interaction with membranes and enabling the sensing and generation of membrane curvature.

In the C2 domain of Smurf2, another Nedd4 family member, conserved

hydrophobic residues (F29 and F30) are responsible for interactions with the HECT domain (see Extended Data Fig. 8a)[4]. Mutation at these residues impairs the interaction between the C2 and HECT domains, resulting in enhanced Smurf2 autoubiquitination by relieving autoinhibition. Consistent with these previous findings, we found that the Nedd4L I37A+F38A mutant, which was not recruited to FCHO2-generated membrane tubules, enhanced autoubiquitination, irrespective of FCHO2 expression (Fig. 2d and Extended Data Fig. 3d). These results suggest that I37 and F38 are critical for interactions with the HECT domain as well as for membrane binding and curvature sensing. This implies that the HECT domain and membranes competitively interact with the C2 domain. Membrane binding of the C2 domain causes catalytic activation by relieving autoinhibition. Thus, the membrane binding of Nedd4L is coupled with its activation.

In vitro activation of Nedd4L by FCHO2-generated membrane curvature

To examine the properties of Nedd4L catalytic activity, we carried out an *in vitro* ubiquitination assay using an αENaC peptide as a substrate. The αENaC peptide possesses a conserved proline-rich motif (PY motif) for interaction with the Nedd4L WW domain, and it is fused with monomeric streptavidin (mSA)[16] to bind to liposomes containing biotinylated phospholipids (biotinylated liposomes)[17] (Extended Data Fig. 9a, b). We found that Ca^{2+} and PS were required for Nedd4L catalytic activity (Fig 4a, b and Extended Data Fig. 10a, b), and that 0.05 μm pore-size liposomes were most effective in stimulating Ca^{2+}- and PS-dependent Nedd4L activity (Fig. 4d and Extended Data Fig. 10d). Thus, the properties of Nedd4L catalytic activity are similar to those of its liposome binding.

We next examined whether membrane localization of mSA-αENaC affects the membrane binding and catalytic activity of Nedd4L. Nedd4L bound only slightly to mSA-αENaC on PS-free (0% PS) liposomes, but the liposome binding was synergistically increased by elevating the PS percentage in liposomes (Fig. 4c and Extended Data Fig. 10c). By contrast, when free biotin competitively inhibited the binding of mSA-αENaC to biotinylated liposomes, the PS-dependent liposome binding of Nedd4L was significantly reduced, resulting in remarkable inhibition of mSA-αENaC ubiquitination (Fig. 4b, c, and Extended Data Fig. 10b, c). Thus, membrane localization of the PY motif is critical for membrane binding and activation of Nedd4L. It is, therefore, likely that the PY motifs on membranes, such as ENaC, play a role in enhancing Nedd4L catalytic activity by potentiating membrane binding through interactions with the WW domain.

We then reconstituted *in vitro* FCHO2-induced recruitment and activation of Nedd4L. When synthetic liposomes (20% PS) or brain-lipid liposomes (20% PS) were used, the FCHO2 BAR domain enhanced the liposome binding of Nedd4L and mSA-αENaC ubiquitination (Fig. 4e, f and Extended Data Fig. 11a, b). This enhancement was lost when the strength of interaction of Nedd4L with liposomes was increased by elevating the PS percentage in liposomes (Folch liposomes, ~50% PS). In contrast to FCHO2, neither amphiphysin1 nor FBP17 enhanced Nedd4L activity (Fig. 4g and Extended Data Fig. 12a). Similarly, tubulation-deficient FCHO2 mutant (L136E) did not enhance Nedd4L activity (Fig. 4h and Extended Data Fig. 12a). These results are in good agreement with those obtained from *in vivo* experiments on FCHO2-induced recruitment and activation of Nedd4L. Electron microscopic analysis revealed that mSA-αENaC-associated liposomes were deformed by membrane-sculpting proteins into tubules with

diameters similar to those of mSA-αENaC-free liposomes (Extended Data Fig. 12b and see Fig. 3c). The diameter of membrane tubules generated by FCHO2 is consistent with that of 0.05 μm pore-size liposomes which are most effective in stimulating Nedd4L activity.

To confirm whether FCHO2-induced recruitment and activation of Nedd4L are mediated by liposomes (i.e., membrane curvature) rather than by protein–protein interactions, we performed two sets of experiments. First, we utilized synthetic liposomes in which 20% PS was replaced with 5% phosphatidylinositol 4,5-bisphosphate [PI(4,5)P_2]. The FCHO2 BAR domain bound to PI(4,5)P_2 as well as PS with high affinity, whereas the Nedd4L C2 domain did not (Extended Data Fig. 13a, b). When synthetic liposomes [5% PI(4,5)P_2] were used, the BAR domain did not stimulate the liposome binding of Nedd4L or mSA-αENaC ubiquitination (Extended Data Fig. 13c, d). Thus, it is unlikely that Nedd4L interacts with the FCHO2 BAR domain on liposomes through protein–protein interactions. Second, we utilized 0.05 μm pore-size liposomes that are most effective in stimulating Nedd4L activity. The FCHO2 BAR domain showed similar binding activity toward 0.8 and 0.05 μm pore-size liposomes (Extended Data Fig. 14a). When 0.8 μm pore-size liposomes were used, the FCHO2 BAR domain enhanced Nedd4L activity (Extended Data Fig. 14b). However, when 0.05 μm pore-size liposomes were used, curvature-stimulated Nedd4L activity was not potentiated by the addition of the FCHO2 BAR domain. These results strongly suggest that FCHO2-induced activation of Nedd4L is mediated by membrane curvature but not by protein–protein interactions.

In summary, we found that FCHO2 is required for Nedd4L-mediated ubiquitination and

endocytosis of ENaC, and that Nedd4L shows co-localization with FCHO2 at CCPs where it likely becomes activated. We also demonstrated that Nedd4L is recruited to and activated by the specific degree of membrane curvature generated by the FCHO2 BAR domain. Furthermore, membrane localization of the PY motif-containing substrate is critical for membrane binding and activation of Nedd4L. Based on the present study, we propose a model for ENaC endocytosis through ubiquitination (Extended Data Fig. 15). First, FCHO2 binds to the plasma membrane and generates a specific degree of membrane curvature. FCHO2 interacts with clathrin adaptor proteins, such as Eps15, and recruits the clathrin machinery for CCP formation[5,18]. Eps15 has Ub-interacting motifs[19]. Nedd4L is subsequently recruited to and activated by FCHO2-generated curved membrane at the rim of nascent CCPs that ENaC enters. ENaC is then ubiquitinated and captured by Eps15 which FCHO2 interacts with. Thus, ubiquitinated ENaC is spatially restricted to CCPs and separated from unmodified ENaC. Overall, our findings suggest that in the early stage of CME, a membrane deformation induced by FCHO2 can program, through both the recruitment and activation of Nedd4L, the gathering of a subclass of cargo molecules in CCPs.

Methods

Construction

Human αENaC, βENaC and γENaC cDNAs were kindly supplied by Dr. H. Kai (Kumamoto University, Kumamoto, Japan)[20]. FLAG-αENaC was constructed by replacing the sequence [amino acid (aa) 169–174, TLVAGS] in the extracellular region

with the FLAG sequence (DYKDDDK) as described previously[21]. This introduction of the epitope tag was carried out by polymerase chain reaction (PCR). FLAG-αENaC, βENaC, and γENaC were subcloned into pTRE-Tight-Hygro, pCAGI-Puro[22], and pCAGI-Bst[23], respectively. pTRE-Tight-Hygro was constructed by inserting the hygromycin-resistance gene into pTRE-Tight (Clontech). FLAG-αENaC was also subcloned into pCAGI-Hygro, which was constructed by replacing the puromycin-resistance gene of pCAGI-Puro with the hygromycin-resistance gene. Human Nedd4L (NM_015277, isoform 3) cDNA was obtained by reverse transcription (RT)-PCR and cloned in pCMV-Myc[22]. Nedd4L was also cloned in pCAGI-puro-EGFP and pGEX-6P-hexahistidine (His6). pGEX-6P-His6 was constructed from pGEX-6P (GE Healthcare) to express an N-terminal GST-tagged, C-terminal His6-tagged protein. pCAGI-puro-EGFP was constructed by subcloning EGFP cDNA into pCAGI-puro to express a C-terminal GFP-tagged protein. The Nedd4L C2 domain (C2, aa 1–160) and C2 domain-deleted mutant (ΔC2, aa 150–955) were subcloned into pCMV-Myc and/or pGEX-6P. Mouse FCHO2 (full length, aa 1–809; BAR domain, aa 1–302) and human FBP17 (BAR domain, aa 1–300) were subcloned into pEGFP-C1 and/or pGEX-6P[18,24]. FCHO2 (aa 1–327) were subcloned into pGEX-6P. Human amphiphysin1 cDNA was obtained by RT-PCR and cloned in pEGFP-N3. Amphiphysin1 (BAR domain, aa 1–377) was then subcloned into pGEX-6P. mTagRFP-T-Clathrin-15 was a gift from Michael Davidson (Addgene plasmid # 58005 ; http://n2t.net/addgene:58005 ; RRID:Addgene_58005)[25]. Human hemagglutinin (HA)-tagged Ub cDNA in pCGN was kindly donated by Dr. M. Nakao (Kumamoto University, Kumamoto, Japan). Ub cDNA was subcloned into pET3a. Human UbcH7 cDNA was obtained by RT-PCR and cloned in pGEX-6P. pET21d-Ube1

was a gift from Cynthia Wolberger (Addgene plasmid # 34965 ; http://n2t.net/addgene:34965 ; RRID:Addgene_34965)[26]. pRSET-mSA was a gift from Sheldon Park (Addgene plasmid # 39860 ; http://n2t.net/addgene:39860 ; RRID:Addgene_39860)[16]. mSA-αENaC was constructed in pRSET-mSA to express a fusion protein of the N-terminal (aa 7–40) and C-terminal (aa 625–659) intracellular regions of αENaC (see Extended Data Fig. 9a). Mutagenesis was performed by PCR using mutated primers and a site-directed mutagenesis kit (Stratagene).

Protein expression and purification

Expression and purification of GST-tagged proteins were performed using standard protocols. His6-tagged proteins were purified with Talon metal affinity resin (Clontech) using the manufacturer's protocol. The GST tag was cleaved off by PreScission protease (GE Healthcare). The GST tag of BAR domains did not inhibit liposome binding or tubulation, whereas the GST tag of Nedd4L inhibited these functions. As FCHO2 (BAR domain, aa 1–302) was easily aggregated by the removal of the GST tag, FCHO2 (aa 1–327) was used instead as a GST-cleaved form of the FCHO2 BAR domain. Full-length Nedd4L (N-terminal GST-tagged, C-terminal His6-tagged) was purified by glutathione–Sepharose (GE Healthcare) column chromatography. The GST tag was cleaved off and the Nedd4L sample was then subjected to Talon metal affinity column chromatography. After the eluate was passed through glutathione–Sepharose beads, the sample was dialyzed against buffer A (20 mM Tris-HCl at pH 7.5, 100 mM KCl, 0.5 mM EDTA, 1 mM DTT, and 20 % sucrose). The Nedd4L sample was stored at −80°C until use. Ub was expressed in *E. coli* strain BL21 (DE3) pJY2 and purified as previously described[27]. His6-

tagged mSA-αENaC was expressed in *E. coli* strain BL21 (DE3) pLysS and purified as previously described[16] with slight modifications. Briefly, the inclusion body was isolated and solubilized in buffer B (50 mM Tris-HCl at pH 8.0 and 6 M guanidine hydrochloride). The sample was then subjected to Talon metal affinity column chromatography. The eluate was added drop by drop to ice-cold refolding buffer (50 mM Tris-HCl at pH 8.0, 150 mM NaCl, 0.15 mg/ml D-biotin, 0.2 mg/ml oxidized glutathione, and 1 mg/ml reduced glutathione) under rapid stirring. The sample was then concentrated using a Centriprep centrifugal filter unit (Millipore) and centrifuged to remove aggregates. The supernatant was dialyzed against buffer C (20 mM Tris-HCl at pH 8.0). The mSA-αENaC sample was further purified by Mono Q anion exchange column chromatography as follows. The sample was applied to a Mono Q 5/50 GL column (GE Healthcare) equilibrated with buffer C. Elution was performed with a 50 ml linear gradient of NaCl (0–200 mM) in buffer C. Fractions of 1 ml each were collected. The active fractions (fraction 18–22) were collected and dialyzed against buffer D (10 mM Tris-HCl at pH 7.5, 100 mM KCl, and 0.5 mM EDTA). The mSA-αENaC sample was stored at −80°C until use.

Antibodies

Rabbit anti-Nedd4L antibody was raised against GST-Nedd4L C2 (aa 1–160). Rabbit anti-FCHO2 antibody was obtained as previously described[18]. The following antibodies were purchased from commercial sources: mouse anti-Myc (9E10) (American Type Culture Collection); mouse anti-FLAG (M2) and mouse anti-α-tubulin (clone DM1A) (Sigma-Aldrich); mouse anti-clathrin heavy chain (BD Biosciences); rabbit anti-GFP (MBL Co.);

rabbit anti-αENaC (Calbiochem); rabbit anti-βENaC (Proteintech); rabbit anti-γENaC (Abcam); mouse anti-Ub antibody P4D1 (Santa Cruz); and secondary antibodies conjugated with Alexa Fluor 488, 594, and 647 (Invitrogen).

Cell culture and transfection

HeLa, HEK293, and COS7 cells were cultured in Dulbecco's modified Eagle medium (DMEM) supplemented with 10% fetal calf serum. HEK293 cells were grown on poly-L-lysine-coated dishes. Transfection was performed by using Lipofectamine 2000 (Invitrogen) according to the manufacturer's protocol.

Generation of stable HeLa cells expressing all three ENaC subunits

HeLa cells were transfected with the pTet-On Advanced vector (Clontech) to develop stable Tet-On cell lines for a doxycycline (Dox)-inducible expression system according to the manufacturer's protocol. Tet-On cells were selected in 0.5 mg/ml G418. Cloned Tet-On cells were then transfected with pCAGI-Bst-γENaC and selected in 4 μg/ml blasticidin (in the presence of G418). Blasticidin-resistant cells were transfected with pCAGI-Puro-βENaC and selected in 1 μg/ml puromycin (in the presence of G418 and blasticidin). Puromycin-resistant cells were finally transfected with pTRE-Tight-Hygro-FLAG-αENaC and cultured in 0.2 mg/ml hygromycin (in the presence of G418, blasticidin, and puromycin). After selection, cells were cloned and maintained in 0.5 mg/ml G418, 0.2 mg/ml hygromycin, 1 μg/ml puromycin, and 2.5 μg/ml blasticidin. FLAG-tagged αENaC expression was induced by treating cells with 1 μg/ml Dox in the presence of 40 μM amiloride overnight. Amiloride was added to prevent cellular Na^+

overload.

Immunofluorescence microscopy

Cells were fixed with 3.7% formaldehyde in phosphate-buffered saline (PBS) at room temperature for 15 min, and then permeabilized with 0.2% Triton X-100 in PBS for 10 min. After blocking with 1% bovine serum albumin (BSA) in PBS, cells were sequentially incubated with primary antibodies and fluorescence-conjugated secondary antibodies at room temperature for 1 h, respectively. Cells were then analyzed with either a fluorescence microscope (BX51; Olympus) or a confocal microscopy system (BX50 and Fluoview FV300; Olympus). A 60 × oil immersion objective (NA = 1.40, Olympus) was used. All comparable images were acquired under identical parameters. To visualize cell-surface FLAG-αENaC in αβγENaC-HeLa cells, cells were incubated with 5 μg/ml anti-FLAG M2 antibody at 4°C for 1 h to prevent internalization. Cells were then fixed, permeabilized, and stained with a secondary antibody. Cells were also sequentially incubated with primary (anti-FCHO2) and secondary antibodies.

RNA interference

Stealth™ double-stranded RNAs were purchased from Invitrogen. siRNA sequences of human FCHO2 and Nedd4L were 5′-CCA CAG AUC UUA GAG UGG AUU AUA A-3′ (corresponding to nucleotides 2048–2072 relative to the start codon) and 5′-GAA GAG UUG CUG GUC UGG CCG UAU U-3′ (corresponding to nucleotides 1778–1802 relative to the start codon), respectively. A double-stranded RNA targeting luciferase (GL-2, 5′-CGU ACG CGG AAU ACU UCG AAA UGU C-3′) was used as a control. HeLa

cells were transfected with 20 nM siRNA using Lipofectamine 2000 according to the manufacturer's protocol. After 24 h, a second transfection was performed, and cells were cultured for 3 days and subjected to various experiments. For rescue experiments, cells were transfected with the intended plasmid at 36 h after the second transfection. After 18 h, cells were fixed and analyzed.

Endocytosis assay

αβγENaC-HeLa cells at approximately 90% confluence in a 10-cm dish were starved with serum-free medium (DMEM containing 1% BSA, 1 μg/ml Dox, and 40 μM amiloride) at 37°C for 4 h. They were then incubated with 5 μg/ml anti-FLAG M2 antibody in 2 ml of DMEM containing 1% BSA at 4°C for 1 h to prevent internalization. After three washes with ice-cold PBS containing 1 mM $MgCl_2$ and 0.1 mM $CaCl_2$ (PBS-CM), endocytosis was allowed by incubating cells in prewarmed DMEM containing 1% BSA at 37°C for the indicated periods of time. Endocytosis was stopped by placing cells on ice and washing them with ice-cold PBS-CM. Antibody bound to the cell surface but not internalized was removed by acid stripping with 0.2 M acetic acid and 0.5 M NaCl solution (pH 2.5). After washing with ice-cold PBS-CM, internalized ENaC was detected by immunoblotting (IB) or immunofluorescence microscopy. For IB, cells were scraped in 1 ml of lysis buffer A (50 mM Tris-HCl at pH 8.0, 150 mM NaCl, 5 mM EDTA, 1% Triton X-100, 1 mM PMSF, 20 μg/ml leupeptin, and 1 μg/ml pepstatin A). Cells were solubilized at 4°C for 1 h on a rotating wheel, and centrifuged at 20,000 × *g* at 4°C for 15 min. Protein G-Sepharose beads (GE Healthcare) were added to the supernatant and incubated at 4°C for 3 h. The beads were then thoroughly washed with lysis buffer A and

boiled in sodium dodecyl sulfate (SDS) sample buffer. The sample was subjected to SDS-polyacrylamide gel electrophoresis (PAGE), followed by IB with anti-ENaC subunit antibodies. Internalization was expressed as a percentage of the initial amount of cell-surface ENaC subunit determined by incubating cells with anti-FLAG antibody at 4°C for 1 h and lysing them without incubation at 37°C or acid stripping. Data represent the mean ± standard error of the mean (SEM) of three independent experiments. For immunofluorescence microscopy, cells were incubated at 37°C for 10 min to allow ENaC endocytosis. After acid stripping, cells were fixed with 3.7% formaldehyde and permeabilized with 0.2% Triton X-100. The antibody-labeled, internalized αENaC was visualized with a fluorescence-conjugated secondary antibody.

Cell surface biotinylation and determination of ENaC ubiquitination

αβγENaC-HeLa cells at approximately 90% confluence in a 10-cm dish were starved with serum-free medium (DMEM containing 1% BSA, 1 μg/ml Dox, and 40 μM amiloride) at 37°C for 4 h, washed three times with ice-cold PBS, and incubated at 4°C for 45 min with 2 ml of 1 mg/ml EZ-link Sulfo-NHS-SS-Biotin (Pierce) in PBS with gentle shaking. Cells. Subsequently, cells were extensively washed with ice-cold Tris-buffered saline, and then scraped into 1 ml of lysis buffer B (50 mM Tris-HCl at pH 7.5, 150 mM NaCl, 5 mM EDTA, 1% Triton X-100, 10 mM N-ethylmaleimide, 1 mM PMSF, 10 μg/ml leupeptin, and 1 μg/ml pepstatin A) containing 40 μM MG132. Cells were solubilized at 4°C for 1 h on a rotating wheel, and centrifuged at 20,000 × *g* at 4°C for 15 min. The supernatant (4 mg of protein) was incubated at 4°C for 3 h with 10 μg of anti-FLAG M2 antibody. Protein G-Sepharose beads (50 μl of 50% slurry) were then added to the sample, which

was incubated at 4°C for 3 h. After beads were thoroughly washed with lysis buffer B containing 40 μM MG132, FLAG-tagged proteins were eluted from the beads with 200 μg/ml FLAG peptide (Sigma-Aldrich) in 0.5 ml of lysis buffer B. After centrifugation, the supernatant was incubated with 25 μl of NeutrAvidin beads (Thermo Scientific) at 4°C overnight. After the beads were thoroughly washed with lysis buffer B, bound proteins were eluted by incubating the beads at 4°C for 1 h with 150 μl of lysis buffer B containing 200 mM DTT. After centrifugation, 5 × SDS sample buffer was added to the supernatant, which was then analyzed by IB.

Liposome preparation

Phospholipids were purchased from commercial sources: phosphatidylcholine (PC, 1,2-dioleoyl-*sn*-glycero-3-phosphocholine), phosphatidylethanolamine (PE, 1,2-dioleoyl-*sn*-glycero-3-phosphoethanolamine), PS (1,2-dioleoyl-*sn*-glycero-3-phospho-L-serine), rhodamine-PE [18:1 L-α-PE-N-(lissamine rhodamine B sulfonyl)], PEG2000-biotin-PE (1,2-distearoyl-*sn*-glycero-3-phosphoethanolamine-N-[biotinyl (polyethyleneglycol)-2000]), porcine brain PS, brain PI(4,5)P_2, and porcine brain total lipid extract were obtained from Avanti Polar Lipids; cholesterol and Folch lipids [bovine brain lipids (Folch Fraction 1)] were obtained from Sigma-Aldrich; X-biotin-PE [N-((6-(biotinoyl)amino)hexanoyl)-1,2-dihexadecanoylsn-glycero-3-phosphoethanolamine] was obtained from Thermo Fisher Scientific; and fluorescein-PE [N-(fluorescein-5-thiocarbamoyl)-1,2-dihexadecanoyl-sn-glycero-3-phosphoethanolamine] was obtained from AAT Bioquest Inc.

Liposomes were prepared using Folch lipids (~50% PS of total lipids), brain lipids (20% PS of total lipids, a mixture of 89.5% porcine brain total lipid extract and 10.5% porcine brain PS), or a synthetic lipid mixture [70% PC, 20% PE, 10% cholesterol (w/w), and varying percentages of PS or PI(4,5)P_2 (with a corresponding reduction in PC)]. Lipid concentrations were monitored by including 1% rhodamine-PE (w/w). To prepare mSA-αENaC–associated liposomes, 2% PEG2000-biotin-PE (w/w) was included. Lipids were dried under nitrogen gas, desiccated for 2 h, and resuspended at 1 mg/ml in lipid buffer (50 mM HEPES-NaOH at pH 7.2, 100 mM KCl, 2 mM $MgCl_2$, and 5 mM EGTA), followed by hydration at 37°C for 1 h. To make liposomes of different sizes, they were subjected to five freeze–thaw cycles and centrifuged at 100,000 × *g* for 15 min. Precipitated liposomes were then resuspended in the same buffer to make a final concentration of 1 mg/ml. They were subjected to extrusion through polycarbonate filter membranes (Avanti Polar Lipids): liposomes were sequentially passed 9 times through a 0.8-µm filter, 21 times through a 0.4-µm filter, 21 times through a 0.2-µm filter, 21 times through a 0.1-µm filter, 21 times through a 0.05-µm filter, and 21 times through a 0.03-µm filter. Instead of extrusion through a 0.03-µm filter, liposomes with the smallest size were also prepared by sonication three times for 5 s with a Branson Sonifier 25 at power level 1. Liposome diameters were examined by transmission electron microscopy.

Co-sedimentation assay

A co-sedimentation assay was performed as described[18] with slight modifications. Briefly, 5–10 µg of protein was incubated at 25°C for 10 min with 0.5 mg/ml liposomes in 100 µl of lipid buffer containing various concentrations of $CaCl_2$ and centrifuged at 165,000 ×

g at 25°C for 15 min. Equal amounts of the supernatants and pellets were subjected to SDS-PAGE, followed by Coomassie brilliant blue (CBB) staining. Proteins were quantified by scanning using ImageJ (NIH). The assay with liposomes of different sizes was performed using NeutrAvidin (Thermo Fisher Scientific Inc) as described[17]. Briefly, Folch liposomes were supplemented with 1% X-biotin-PE and 1% rhodamine-PE, subjected to extrusion through filter membranes, and then sonicated. Purified Nedd4L protein (10 μg) was incubated with 0.2 mg/ml liposomes in 100 μl of lipid buffer containing 2mM $CaCl_2$ (0.1 μM Ca^{2+}). The sample was then incubated with 2 μg of NeutrAvidin and ultracentrifuged. Both total and supernatant fluorescence were measured. The percentage of precipitated liposomes of each size was estimated to be ~100%.

The assay with mSA-αENaC–associated liposomes was performed as follows. Liposomes were prepared from a synthetic lipid mixture [various percentages of PS or 5% $PI(4,5)P_2$] or brain lipids supplemented with 2% PEG2000-biotin-PE and 1% rhodamine-PE. The liposomes (10 μg) were incubated with purified mSA-αENaC protein (35 pmol) at 4°C for 10 min in 25 μl of lipid buffer. The sample was then incubated at 25°C for 10 min with 0.07 μM (8 μg/ml) Nedd4L and/or 1.4 μM BAR domains in 50 μl of ubiquitination buffer (50 mM HEPES-NaOH at pH 7.2, 100 mM KCl, 2 mM $MgCl_2$, 5 mM EGTA, and 0.1 mM DTT) containing 4 mM $CaCl_2$ (0.7 μM Ca^{2+}). Subsequently, the sample was subjected to ultracentrifugation. Equal amounts of the total samples and pellets were subjected to SDS-PAGE, followed by CBB staining and IB. The chemiluminescence intensity was quantified by scanning using ImageJ (NIH).

The assay with mSA-αENaC-associated liposomes (0.05 μm pore-size) was done as follows. Liposomes were prepared from brain lipids supplemented with 2%

PEG2000-biotin-PE, 1% rhodamine-PE, and 0.5% fluorescein-PE (w/w) and extruded through membrane filters. To precipitate liposomes, the sample (50 μl) was first incubated with 1 μg of anti-fluorescein goat antibody (Novus Biologicals) at room temperature for 1 h and then incubated with 0.5 μg of protein A/G/L (BioVision) at room temperature for 1 h. Subsequently, the sample was centrifuged at 165,000 × *g* at 25°C for 15 min. Equal amounts of the supernatants and pellets were subjected to SDS-PAGE, followed by CBB staining and IB. The percentage of precipitated liposomes was estimated to be ~100%.

Calculation of free Ca^{2+} concentrations

At 1.0, 2.0, 3.0, 3.5, 4.0, 4.5, and 4.9 mM $CaCl_2$ in lipid buffer, free Ca^{2+} concentrations were calculated to be 0.04, 0.1, 0.3, 0.4, 0.7, 1.6, and 8.1 μM, respectively, as determined by the Ca-Mg-ATP-EGTA Calculator v1.0 using constants from the NIST database #46 v8. At 1.0, 2.0, 3.0, 3.5, 4.0, 4.5, and 4.9 mM $CaCl_2$ in ubiquitination buffer, free Ca^{2+} concentrations were calculated to be 0.04, 0.1, 0.2, 0.4, 0.7, 1.4, and 6.7 μM, respectively.

***In vitro* tubulation assay**

An *in vitro* tubulation assay was performed as described[18,24] with slight modifications. Briefly, liposomes were prepared from Folch lipids supplemented with 1 % rhodamine-PE. The liposomes (0.2 mg/ml liposomes) were incubated with the Nedd4L C2 domain (4.5 μM) or BAR domains (1.4 μM) at 25°C for 10 min in lipid buffer containing 3 mM $CaCl_2$ (0.3 μM Ca^{2+}). The sample was examined by fluorescence microscopy or electron microscopy. The tubulation assay with mSA-αENaC-associated liposomes was performed using the sample mixture utilized in the co-sedimentation assay in which mSA-

αENaC-associated liposomes (brain-lipid liposomes) were used.

Negative-staining electron microscopy

Negative-staining transmission electron microscopy was performed as described[28]. Box and whisker plots were used to represent the distribution of liposome diameters (n = 50).

***In vivo* ubiquitination assay**

HEK293 cells were used, because they formed membrane tubules upon FCHO2 expression more efficiently than did COS7 cells: 91 ± 5% of HEK293 cells *vs.* 32 ± 4% of COS7 cells. HEK293 cells at approximately 90% confluence on a 6-well plate were transfected with 0.8 μg of pCMV-Myc-Nedd4L, 1.6 μg of pEGFP-BAR domain, and 1.6 μg of pCGN-HA-Ub. In some experiments, cells were transfected with various doses (0–1.5 μg) of pCMV-Myc-Nedd4L, 1.5 μg of pEGFP-FCHO2 BAR domain, 1 μg of pCGN-HA-Ub, and 0.5 μg of pCAGI-Hygro-FLAG-αENaC. Total transfected cDNA amount was held constant using empty pCMV-Myc vector. Amiloride (40 μM) was added to the medium when αENaC cDNA was transfected. At 21 h after transfection, cells were washed with PBS and incubated with serum-free DMEM containing 1% BSA. After 3 h incubation, 10 μM MG132 was added to the medium. After further 4 h incubation, cells were solubilized in 150 μl of lysis buffer C (50 mM Tris-HCl at pH 7.5, 150 mM NaCl, 5 mM EDTA, 10 mM N-ethylmaleimide, 1 mM PMSF, 10 μg/ml leupeptin, and 1μg/ml pepstatin A) containing 1% SDS. After boiling, the sample was sonicated and then centrifuged at 20,000 × *g* for 15 min. The supernatant was diluted 10-fold with lysis buffer C containing 1% Triton X-100 and then incubated at 4°C for 3 h with either anti-

Myc or anti-FLAG M2 antibody. Protein G-Sepharose beads were added to the sample, which was then incubated at 4°C for 3 h. After the beads were thoroughly washed with lysis buffer C containing 1% Triton X-100, bound proteins were eluted by boiling in SDS sample buffer for 5 min. These proteins were then subjected to SDS-PAGE, followed by IB.

In vitro ubiquitination assay

mSA-αENaC-associated liposomes were made by incubating liposomes (10 μg) with mSA-αENaC (35 pmol) in 25 μl of lipid buffer, as described for the co-sedimentation assay. They were then incubated at 25°C for 10 min with 0.07 μM Nedd4L, 0.04 μM E1 (Ube1), 0.7 μM E2 (UbcH7), 7 μM Ub, and various concentrations of BAR domains in 50 μl of ubiquitination buffer containing 4 mM $CaCl_2$ (0.7 μM Ca^{2+}) and 2 mM ATP. Where indicated, various concentrations of $CaCl_2$ were used. The ubiquitination reaction was started by adding ATP and stopped by adding 10 μl of 6 × SDS sample. The sample was then boiled, subjected to SDS-PAGE, and immunoblotted with anti-Ub and anti-αENaC antibodies. The chemiluminescence intensity was quantified by scanning using ImageJ (NIH).

Other procedures

Stripping immunoblots for re-probing was carried out with the WB Stripping Solution Strong (Nacalai Tesque) according to the manufacturer's protocol. Protein concentrations were quantified with BSA as a reference protein by the Bradford method (Bio-Rad) or the BCA method (Thermo Fisher Scientific). SDS-PAGE was performed as described[29].

Statistical analysis

All experiments were performed at least in triplicate and representative results are shown. Data are shown as the mean ± SEM. Student's tests were used to evaluate statistical significances between different treatment groups.

References

1. Rotin, D. & Kumar, S. Physiological functions of the HECT family of ubiquitin ligases. *Nat. Rev. Mol. Cell Biol.* **10**, 398–409 (2009).
2. Rossier, B. C. Epithelial sodium channel (ENaC) and the control of blood pressure. *Curr. Opin. Pharmacol.* **15**, 33–46 (2014).
3. Wang, J. *et al.* Calcium activates Nedd4 E3 ubiquitin ligases by releasing the C2 domain-mediated auto-inhibition. *J. Biol. Chem.* **285**, 12279–12288 (2010).
4. Wiesner, S. *et al.* Autoinhibition of the HECT-type ubiquitin ligase Smurf2 through its C2 domain. *Cell* **130**, 651–862 (2007).
5. Henne, W. M. *et al.* FCHo proteins are nucleators of clathrin-mediated endocytosis. *Science* **328**, 1281–1284 (2010).
6. Frost, A. *et al.* Structural basis of membrane invagination by F-BAR domains. *Cell* **132**, 807–817 (2008).
7. Suetsugu, S., Toyooka, K. & Senju, Y. Subcellular membrane curvature mediated by the BAR domain superfamily proteins. *Semin. Cell Dev. Biol.* **21**, 340–349 (2009).

8. Takei, K., Slepnev, V. I., Haucke, V. & De Camilli, P. Functional partnership between amphiphysin and dynamin in clathrin-mediated endocytosis. *Nat. Cell Biol.* **1**, 33–39 (1999).

9. Peter, B. J. *et al.* BAR domains as sensors of membrane curvature: the amphiphysin BAR structure. *Science* **303**, 495–499 (2004).

10. Yin, Y., Arkhipov, A. & Schulten, K. Simulations of membrane tubulation by lattices of amphiphysin N-BAR domains. *Structure* **17**, 882–892 (2009).

11. Henne, W. M. *et al.* Structure and analysis of FCHo2 F-BAR domain: a dimerizing and membrane recruitment module that effects membrane curvature. *Structure* **15**, 839–852 (2007).

12. Takano, K., Toyooka, K. & Suetsugu, S. EFC/F-BAR proteins and the N-WASP–WIP complex induce membrane curvature-dependent actin polymerization. *EMBO J.* **27**, 2817–2828 (2008).

13. McMahon, H. T. & Boucrot, E. Molecular mechanism and physiological functions of clathrin-mediated endocytosis. *Nat. Rev. Mol. Cell Biol.* **12**, 517–533 (2011).

14. Zhou, R., Patel, S. V. & Snyder, P. M. Nedd4-2 catalyzes ubiquitination and degradation of cell surface ENaC. *J. Biol. Chem.* **282**, 20207–20212 (2007).

15. Martens, S., Kozlov, M. M. & McMahon, H. T. How synaptotagmin promotes membrane fusion. *Science* **316**, 1205–1208 (2007).

16. Lim, K. H., Huang, H., Pralle, A. & Park, S. Stable, high-affinity streptavidin monomer for protein labeling and monovalent biotin detection. *Biotechnol. Bioeng.* **110**, 57–67 (2013).

17. Sakamoto, Y., Kikuchi, K., Umeda, K. & Nakanishi, H. Effects of various spacers between biotin and the phospholipid headgroup on immobilization and sedimentation of biotinylated phospholipid-containing liposomes facilitated by avidin-biotin interactions. *J. Biochem.* **162**, 221–226 (2017).

18. Uezu, A. *et al.* Characterization of the EFC/F-BAR domain protein, FCHO2. *Genes Cells* **16**, 868–878 (2011).

19. Di Fiore, P. P., Polo, S. & Hofmann, K. When ubiquitin meets ubiquitin receptors: a signalling connection. *Nat. Rev. Mol. Cell Biol.* **4**, 491–497 (2003).

20. Sugahara, T. *et al.* Calreticulin positively regulates the expression and function of epithelial sodium channel. *Exp. Cell Res.* **315**, 3294–3300 (2009).

21. Firsov, D. *et al.* Cell surface expression of the epithelial Na channel and a mutant causing Liddle syndrome: a quantitative approach. *Proc. Natl. Acad. Sci. U. S. A.* **93**, 15370–15375 (1996).

22. Miyahara, M. *et al.* Interaction of nectin with afadin is necessary for its clustering at cell-cell contact sites but not for its cis dimerization or trans interaction. *J. Biol. Chem.* **275**, 613–618 (2000).

23. Umeda, K. *et al.* ZO-1 and ZO-2 independently determine where claudins are polymerized in tight-junction strand formation. *Cell* **126**, 741–754 (2006).

24. Tsujita, K. *et al.* Coordination between the actin cytoskeleton and membrane deformation by a novel membrane tubulation domain of PCH proteins is involved in endocytosis. *J. Cell Biol.* **172**, 269–279 (2006).

25. Shaner, N. C. *et al.* Improving the photostability of bright monomeric orange and red fluorescent proteins. *Nat. Methods* **5**, 545–551 (2008).

26. Berndsen, C. E. & Wolberger, C. A spectrophotometric assay for conjugation of ubiquitin and ubiquitin-like proteins. *Anal. Biochem.* **418**, 102–110 (2011).

27. Pickart, C. M. & Raasi, S. Controlled synthesis of polyubiquitin chains. *Methods Enzymol.* **399**, 21–36 (2005).

28. Shimada, A. *et al.* Curved EFC/F-BAR-domain dimers are joined end to end into a filament for membrane invagination in endocytosis. *Cell* **129**, 761–772 (2007).

29. Laemmli, U. K. Cleavage of structural proteins during the assembly of the head of bacteriophage T4. *Nature* **227**, 680–685 (1970).

30. Hughey, R. P. *et al.* Maturation of the epithelial Na+ channel involves proteolytic processing of the alpha- and gamma-subunits. *J. Biol. Chem.* **278**, 37073–37082 (2003).

Acknowledgments

We thank Drs. H. Kai and M. Nakao for kindly providing us with ENaC and Ub cDNAs, respectively. We are also grateful to Dr. T. Takenawa (Kobe University, Kobe, Japan) for helpful discussions. This work was partly carried out at the Institute of Molecular Embryology and Genetics, the Gene Technology Centre, and Research Facilities of the School of Medicine, Kumamoto University. This study was supported by JSPS KAKENHI Grant Numbers 19K06643 (to H.N.), 19K06544 (to Y.S.), and Setsuro Fujii Memorial, The Osaka Foundation for Promotion of Fundamental Medical Research (to Y.S.) and by grants from the Mochida Memorial Foundation, the Takeda Science Foundation, and the Uehara Memorial Foundation (to K.K.).

Author Contributions

Y.S., A.U., and H.N. conceived and designed the project with contributions from K.K.; Y.S., A.U., and H.N. performed experiments; S.S. contributed to providing the cDNAs of FBP17 and amphiphysin1 and to analyzing tubulation by electron microscopy; Y.S., A.U., K.K., and H.N. analyzed data and interpreted results; Y.S. and H.N. wrote the manuscript with contributions from K.K.

Competing interests

The authors declare no competing interests.

Fig. 1

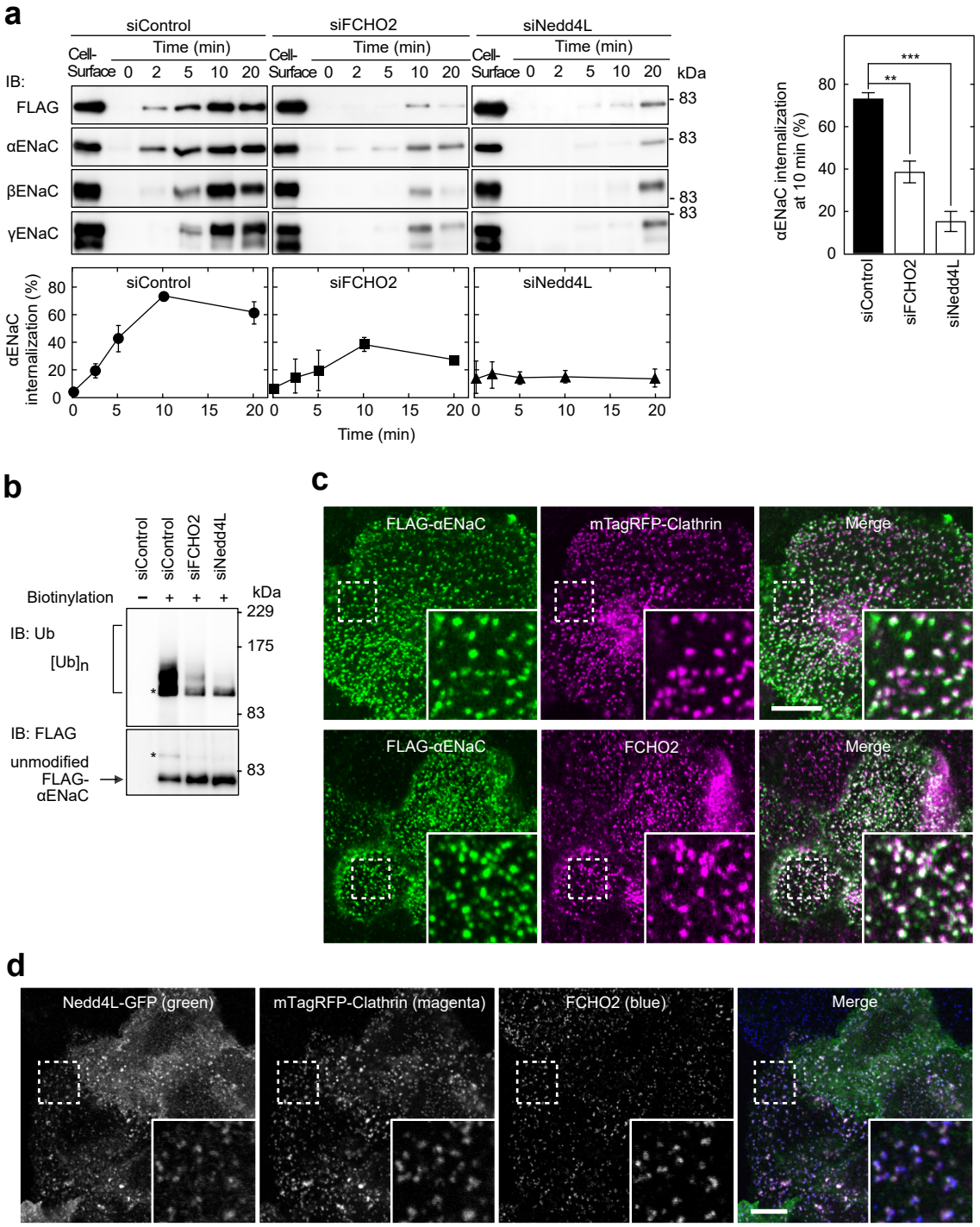

Fig. 1 | FCHO2 is required for Nedd4L-mediated ubiquitination and endocytosis of ENaC. a, ENaC endocytosis. αβγENaC-HeLa cells treated with each siRNA were subjected to an endocytosis assay using anti-FLAG antibody. A FLAG tag was introduced into the extracellular region of αENaC. Initial cell-surface and internalized ENaC subunits were detected by immunoblotting (IB) (upper panels) and quantified (bottom panels and right panel). Internalization was expressed as a percentage of the initial amount of cell-surface αENaC. Data are shown as the mean ± S.E.M of three independent experiments. **, $P < 0.01$; ***, $P < 0.001$ (the Student's *t*-test). **b,** ENaC ubiquitination. Cell-surface αENaC was biotinylated and sequentially precipitated with anti-FLAG antibody and then avidin beads. Samples were analyzed by IB. Asterisks indicate the same band of ubiquitinated FLAG-αENaC. **c,** Co-localization of cell-surface ENaC with FCHO2 at clathrin-coated pits. mTagRFP-clathrin was expressed in αβγENaC-HeLa cells. Cell-surface αENaC was labeled by incubating with anti-FLAG antibody at 4°C. Cells were then fixed and stained with anti-FCHO2 antibody. Insets represent enlarged images of the dashed boxes. Scale bar, 10 μm. **d,** Co-localization of Nedd4L with FCHO2 at clathrin-coated pits. Nedd4L-GFP and mTagRFP-clathrin were co-expressed in HeLa cells. Cells were then fixed and stained with anti-FCHO2 antibody. Insets represent enlarged images of the dashed boxes. Scale bar, 10 μm.

Fig. 2

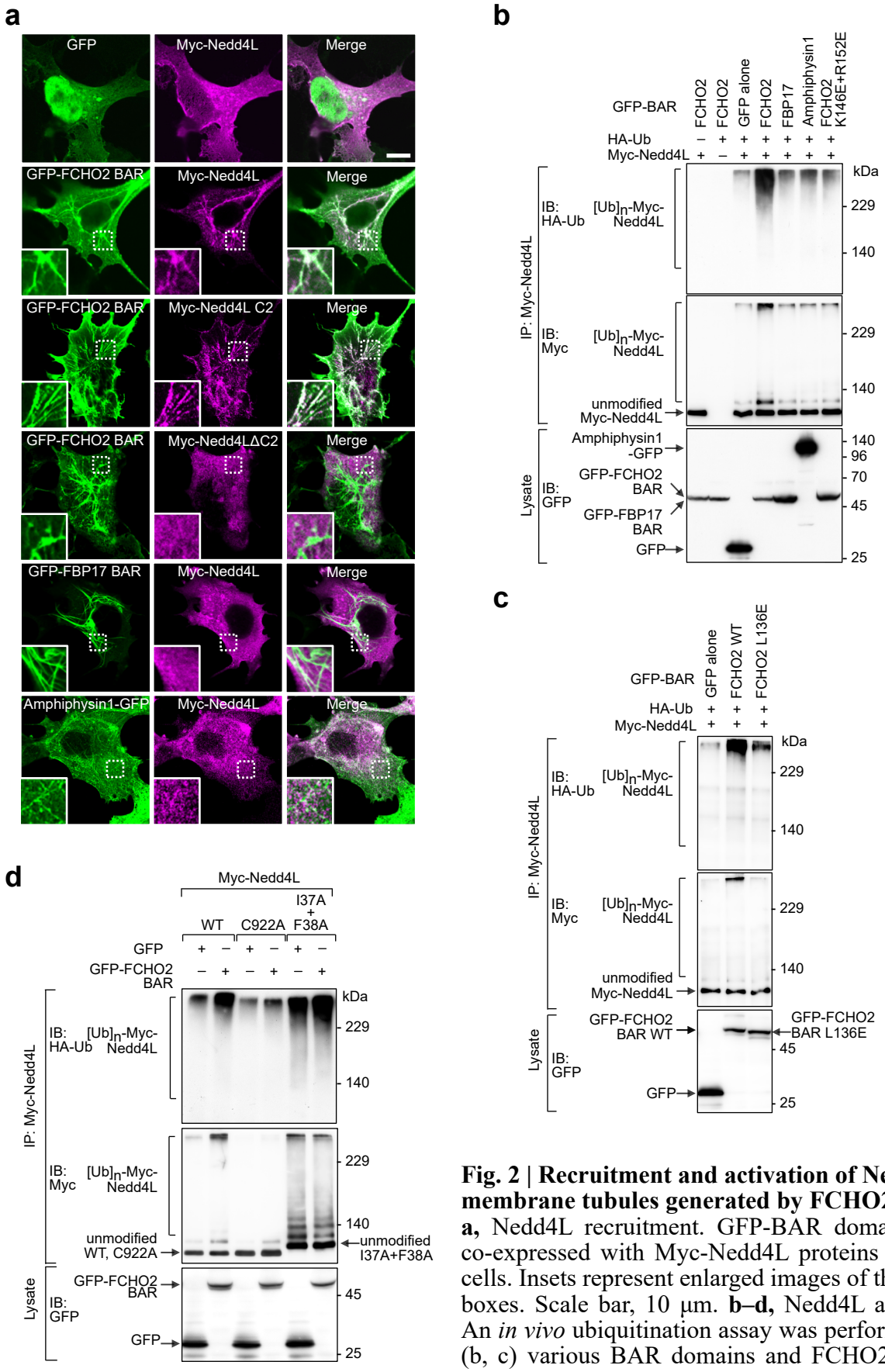

Fig. 2 | Recruitment and activation of Nedd4L by membrane tubules generated by FCHO2 in cells. a, Nedd4L recruitment. GFP-BAR domains were co-expressed with Myc-Nedd4L proteins in COS7 cells. Insets represent enlarged images of the dashed boxes. Scale bar, 10 μm. **b–d,** Nedd4L activation. An *in vivo* ubiquitination assay was performed with (b, c) various BAR domains and FCHO2 mutants and (d) Nedd4L mutants. GFP-BAR domains were co-expressed with Myc-Nedd4L proteins and HA-tagged Ub in HEK293 cells. Cell lysates were subjected to immunoprecipitation (IP). Samples were analyzed by IB. WT, wild type.

Fig. 3

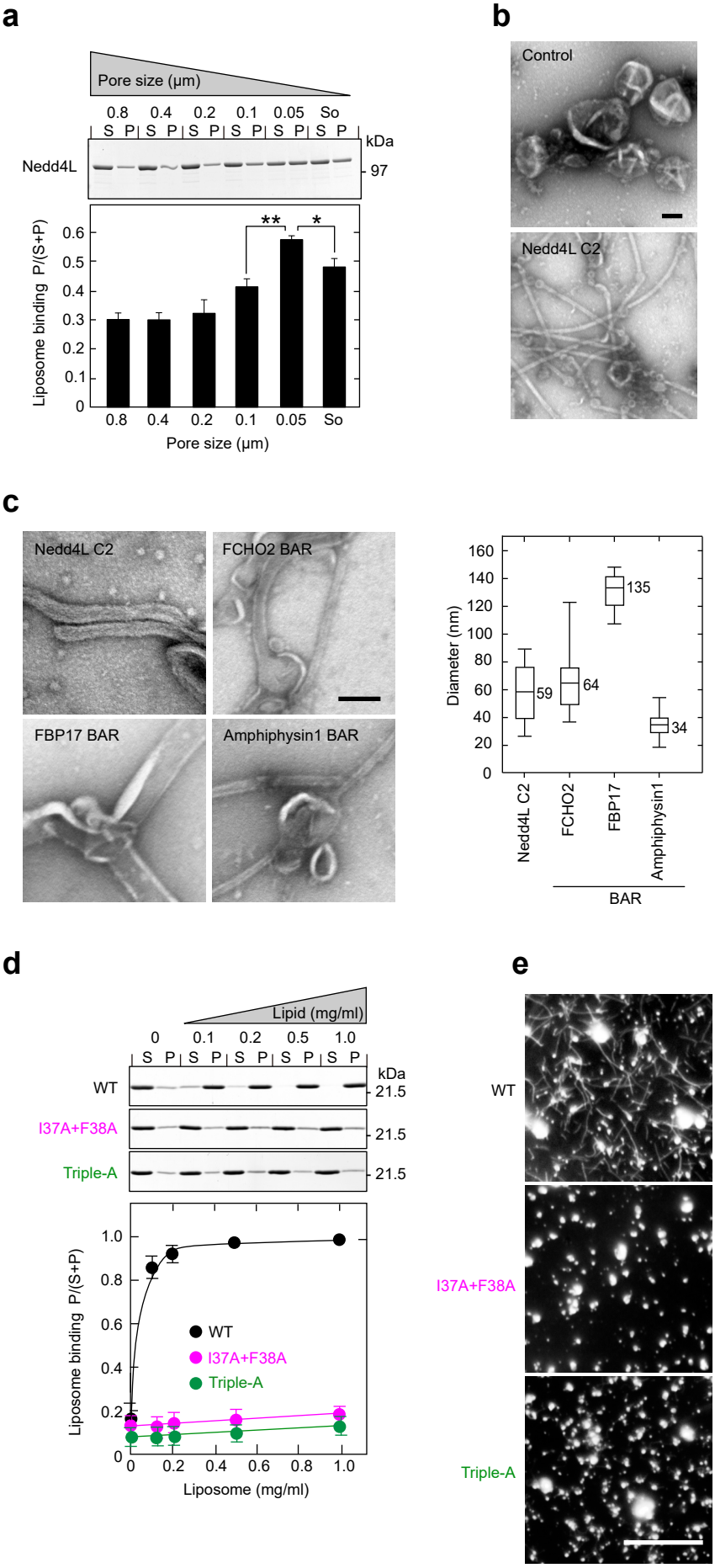

Fig. 3 | Sensing and generation of membrane curvature by Nedd4L. Co-sedimentation (a, d) and *in vitro* tubulation (b, c, e) assays were performed using Folch liposomes at (a) 0.1 μM and (b-e) 0.3 μM Ca^{2+}. **a,** Preference of Nedd4L for a specific degree of membrane curvature. The assay was performed with full-length Nedd4L using liposomes of different sizes which were prepared by extrusion through the indicated pore sizes. The supernatant (S) and pellet (P) were subjected to sodium dodecyl sulfate (SDS)-polyacrylamide gel electrophoresis (PAGE), followed by Coomassie brilliant blue (CBB) staining (upper panel). Bottom panel, quantitative analysis. So, sonication. Data are shown as the mean ± S.E.M of three independent experiments. *, $P < 0.05$; **, $P < 0.01$ (the Student's *t*-test). **b,** Curvature generation by Nedd4L. The assay was performed with the Nedd4L C2 domain. Samples were examined by electron microscopy. Scale bar, 200 nm. **c,** The degree of membrane curvature generated by Nedd4L is consistent with that generated by FCHO2. The assay was performed with the indicated protein. Left panel, electron microscopic image. Scale bar, 200 nm. Right panel, distribution of tubule diameters. **d,** Inability of Nedd4L C2 domain mutants to bind membranes. The assay was performed with Nedd4L C2 domain mutants using various concentrations of liposomes. The supernatant (S) and pellet (P) were subjected to SDS-PAGE, followed by CBB staining (upper panel). Bottom panel, quantitative analysis. **e**, Inability of Nedd4L C2 domain mutants to generate membrane curvature. The assay was performed with Nedd4L C2 domain mutants. Samples were examined by fluorescence microscopy. Scale bar, 10 μm.

Fig. 4

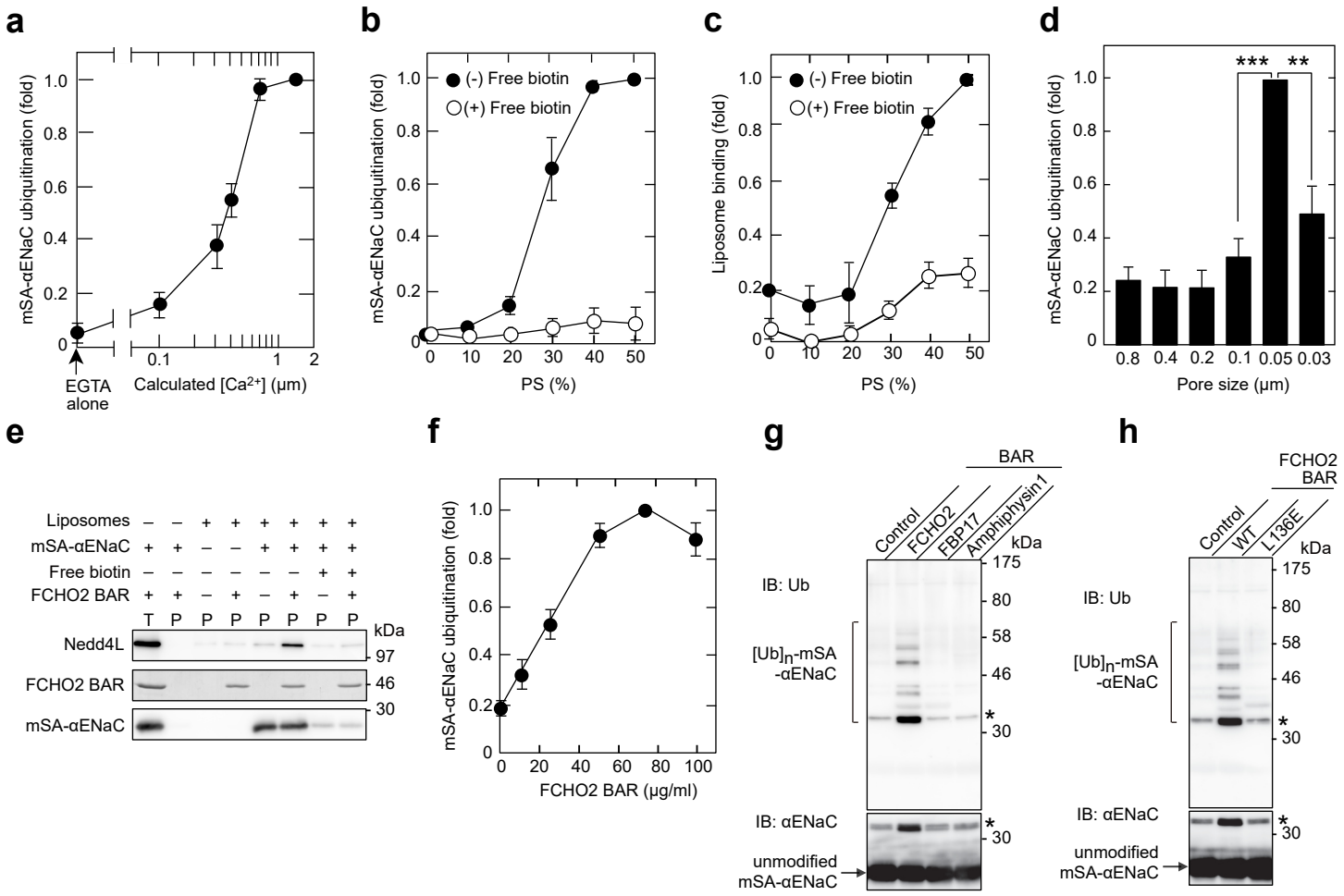

Fig. 4 | Recruitment and activation of Nedd4L by FCHO2-generated membrane curvature *in vitro*. Liposomes supplemented with biotinylated phospholipids were incubated with mSA-αENaC. Samples were mixed with Nedd4L in the presence or absence of BAR domains. Mixtures were subjected to ubiquitination (a, b, d, f-h) and co-sedimentation (c, e) assays. These assays were performed with (a) Folch liposomes at various Ca^{2+} concentrations, with (b, c) synthetic liposomes (various percentages of PS) at 0.7 μM Ca^{2+}, and with (d-h) brain-lipid liposomes at 0.7 μM Ca^{2+}. Ubiquitination and liposome binding were quantified by scanning and expressed as ratios to maximum levels. **a,** Ca^{2+}-dependent Nedd4L activity. **b, c**, Membrane localization of mSA-αENaC enhances the PS-dependent catalytic activity and membrane binding of Nedd4L. Assays were performed in the presence or absence of 40 μM biotin. **d,** Nedd4L activity is predominantly stimulated by the specific degree of membrane curvature. The assay was performed using liposomes of different sizes which were prepared by extrusion through the indicated pore sizes. Data are shown as the mean ± S.E.M of three independent experiments. **, $P < 0.01$; ***, $P < 0.001$ (the Student's *t*-test). **e,** FCHO2-induced recruitment of Nedd4L. The assay was performed with the FCHO2 BAR domain (1.4 μM, 50 μg/ml) in the presence or absence of biotin. The total sample (T) and pellets (P) were subjected to SDS-PAGE, followed by CBB staining (FCHO2 BAR) and IB (Nedd4L and mSA-αENaC). **f,** FCHO2-induced activation of Nedd4L. The assay was performed with various concentrations of the FCHO2 BAR domain. **g, h,** Specificity of BAR domains and effect of an FCHO2 mutant. The assay was performed with (g) various BAR domains and (h) an FCHO2 mutant (1.4 μM each). Samples were analyzed by IB.

Extended Data Fig. 1

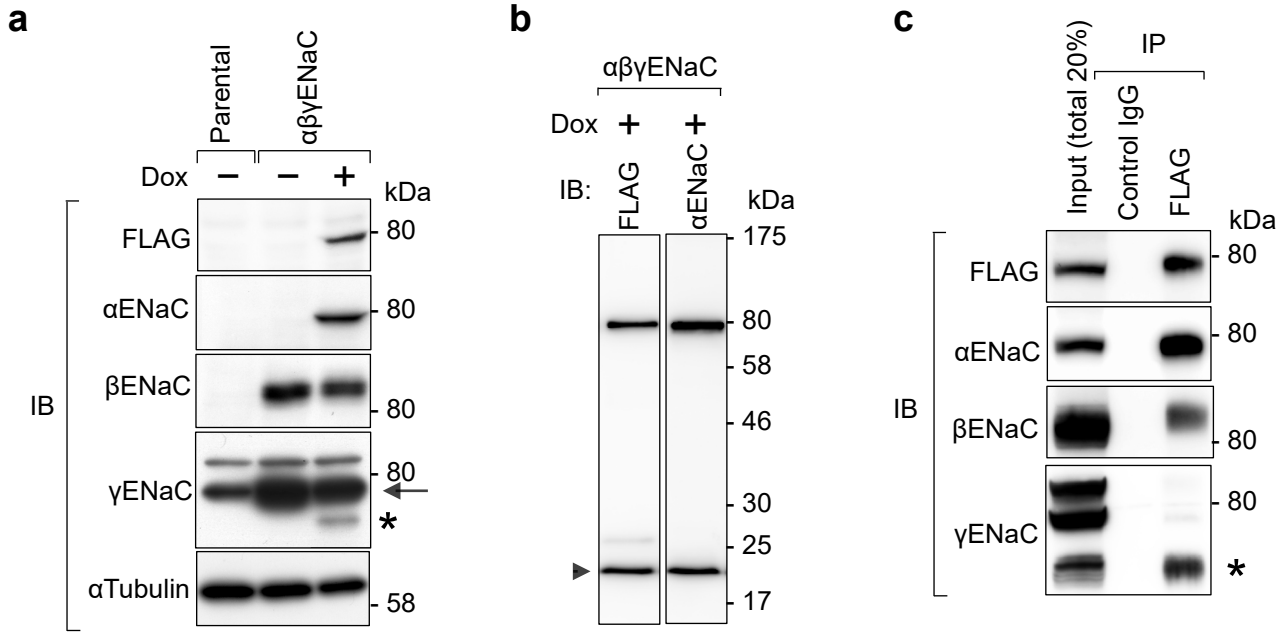

Extended Data Fig. 1 | Expression of ENaC subunits in αβγENaC-HeLa cells. a, b, Doxycycline (Dox)-induced expression of αENaC. αβγENaC-HeLa cells were cultured overnight in the presence or absence of Dox. The lysates of parental HeLa and αβγENaC-HeLa cells were subjected to immunoblotting (IB). (a) 7.5% gel. (b) Gradient gel (5-20%). Anti-γENaC antibody cross-reacted with two bands of endogenous proteins in parental HeLa cells, the lower band of which overlapped with γENaC (arrow) in αβγENaC-HeLa cells. Upon Dox-induced αENaC expression, an additional 70-kDa γENaC band (asterisk) was detected. It has been shown that co-expression of all three subunits induces ENaC maturation, including proteolytic cleavage of αENaC and γENaC[30]. The 70-kDa γENaC band is likely a cleavage product comprising the C-terminal region. The 20-kDa αENaC band (arrowhead) is likely a cleavage product comprising the N-terminal region. **c,** Association of the α, β, and γ subunits. When αENaC was immunoprecipitated with anti-FLAG antibody from αβγENaC-HeLa cells treated with Dox, βENaC and γENaC were co-precipitated.

Extended Data Fig. 2

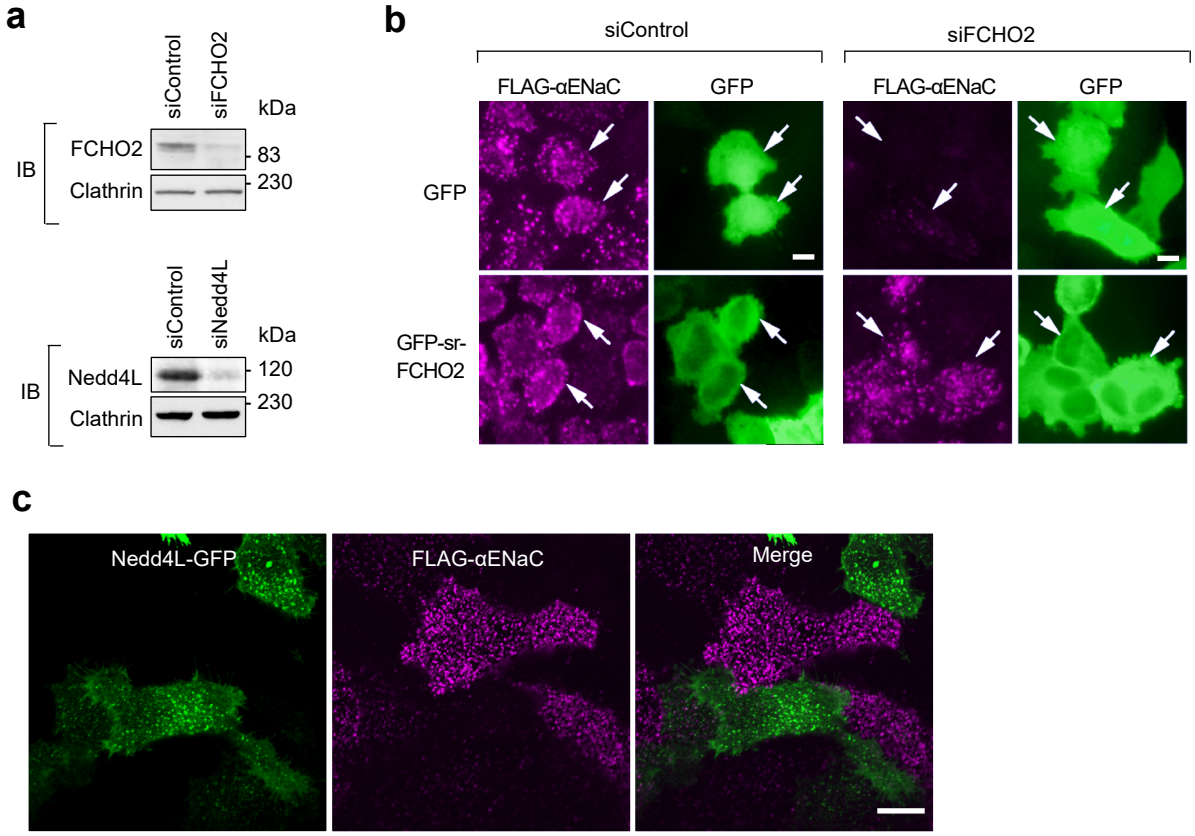

Extended Data Fig. 2 | ENaC endocytosis in αβγENaC-HeLa cells. **a,** Knockdown of FCHO2 or Nedd4L by siRNA. Samples were analyzed by IB. **b,** Restoration of αENaC endocytosis by FCHO2 re-expression in knockdown cells. Cells were transfected with the indicated siRNA and GFP construct and subjected to an endocytosis assay, followed by immunofluorescence microscopy. Arrows indicate cells expressing GFP-tagged proteins. Scale bars, 10 μm. **c,** Failure to detect the co-localization of cell-surface αENaC with Nedd4L. Cells were transfected with Nedd4L-GFP. Cell-surface αENaC were labeled by incubating with anti-FLAG antibody at 4°C, followed by immunofluorescence microscopy. Scale bar, 10 μm.

Extended Data Fig. 3

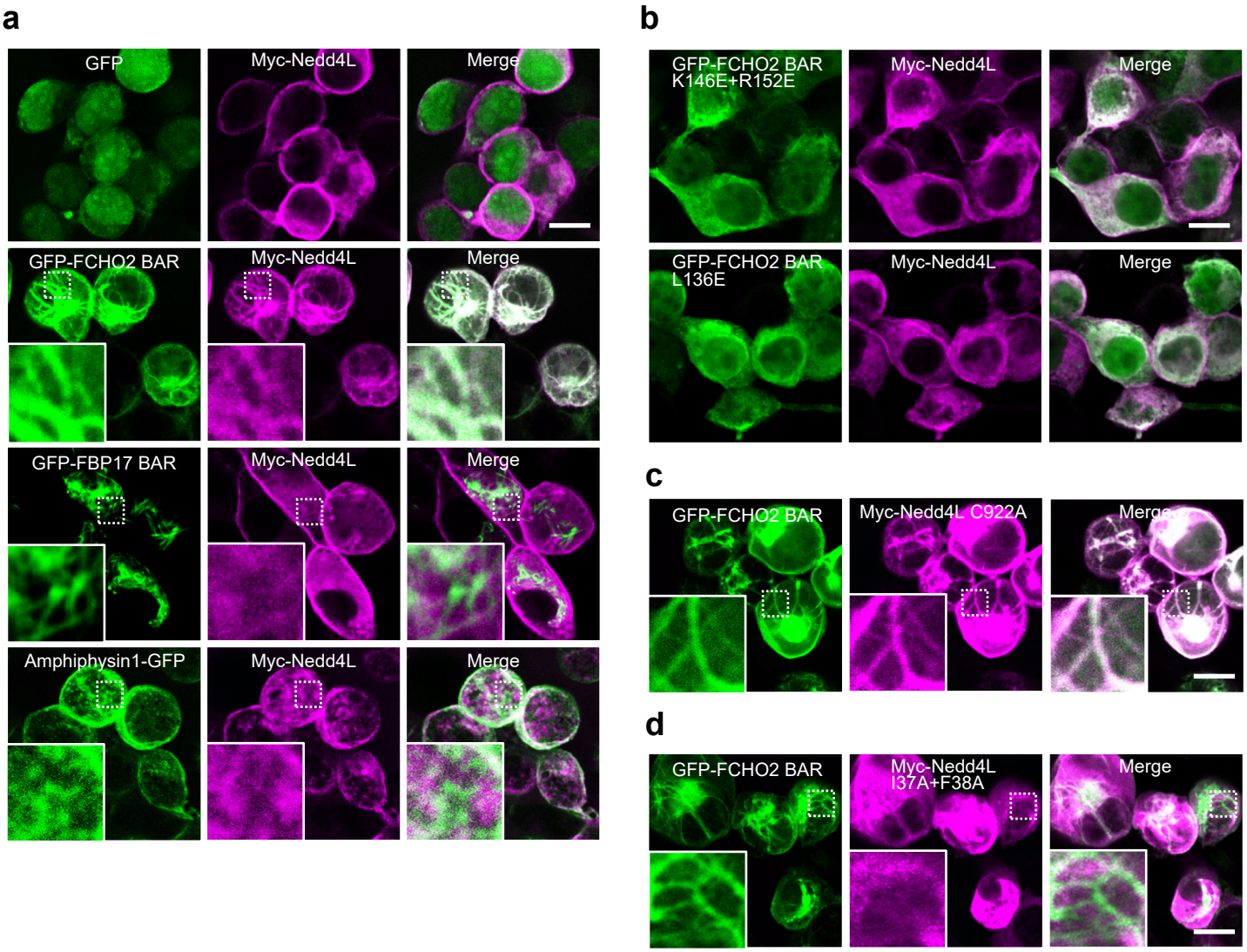

Extended Data Fig. 3 | Recruitment of Nedd4L to membrane tubules generated by FCHO2. GFP-BAR domains were co-expressed with Myc-Nedd4L proteins in HEK293 cells. Cells were serum-starved and subjected to immunofluorescence microscopy. Insets represent enlarged images of the dashed boxes. Scale bars, 10 μm. **a,** Specificity of BAR domains. **b,** Inability of FCHO2 mutants to generate membrane tubules. **c, d,** Effects of Nedd4L mutations on the recruitment to membrane tubules.

Extended Data Fig. 4

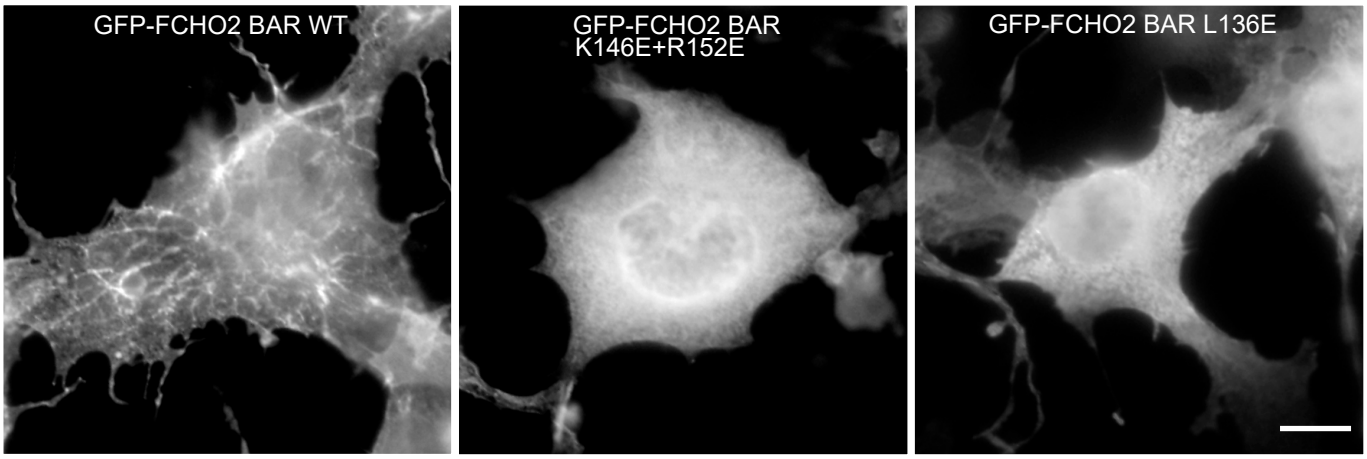

Extended Data Fig. 4 | Inability of FCHO2 mutants to generate membrane tubules. GFP-FCHO2 BAR domain [wild type (WT) or mutant] was expressed in COS7 cells. Cells were then subjected to immunofluorescence microscopy. Scale bar, 10 μm.

Extended Data Fig. 5

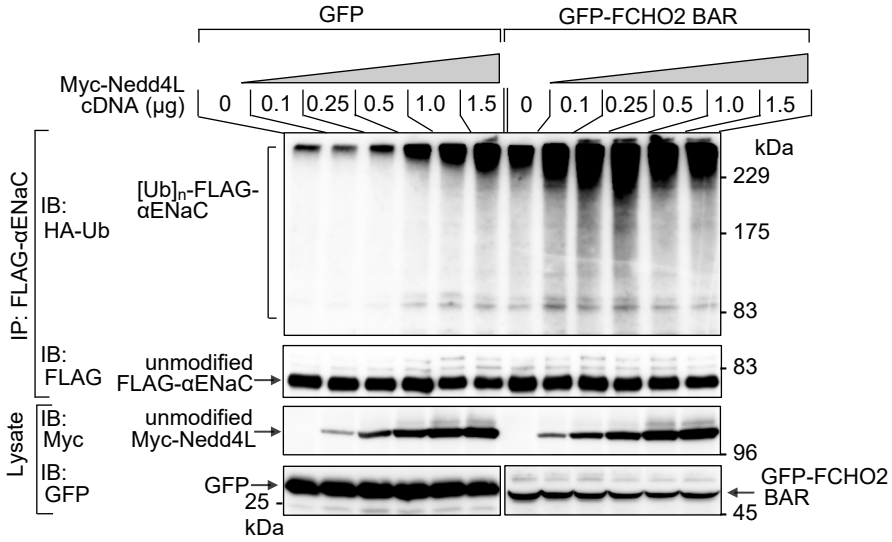

Extended Data Fig. 5 | Stimulation of Nedd4L-mediated αENaC ubiquitination by FCHO2 in cells. An *in vivo* ubiquitination assay was performed with various concentrations of Myc-Nedd4L using FLAG-αENaC as a substrate in the presence or absence of GFP-FCHO2 BAR domain. Cell lysates were subjected to immunoprecipitation (IP). Samples were analyzed by IB.

Extended Data Fig. 6

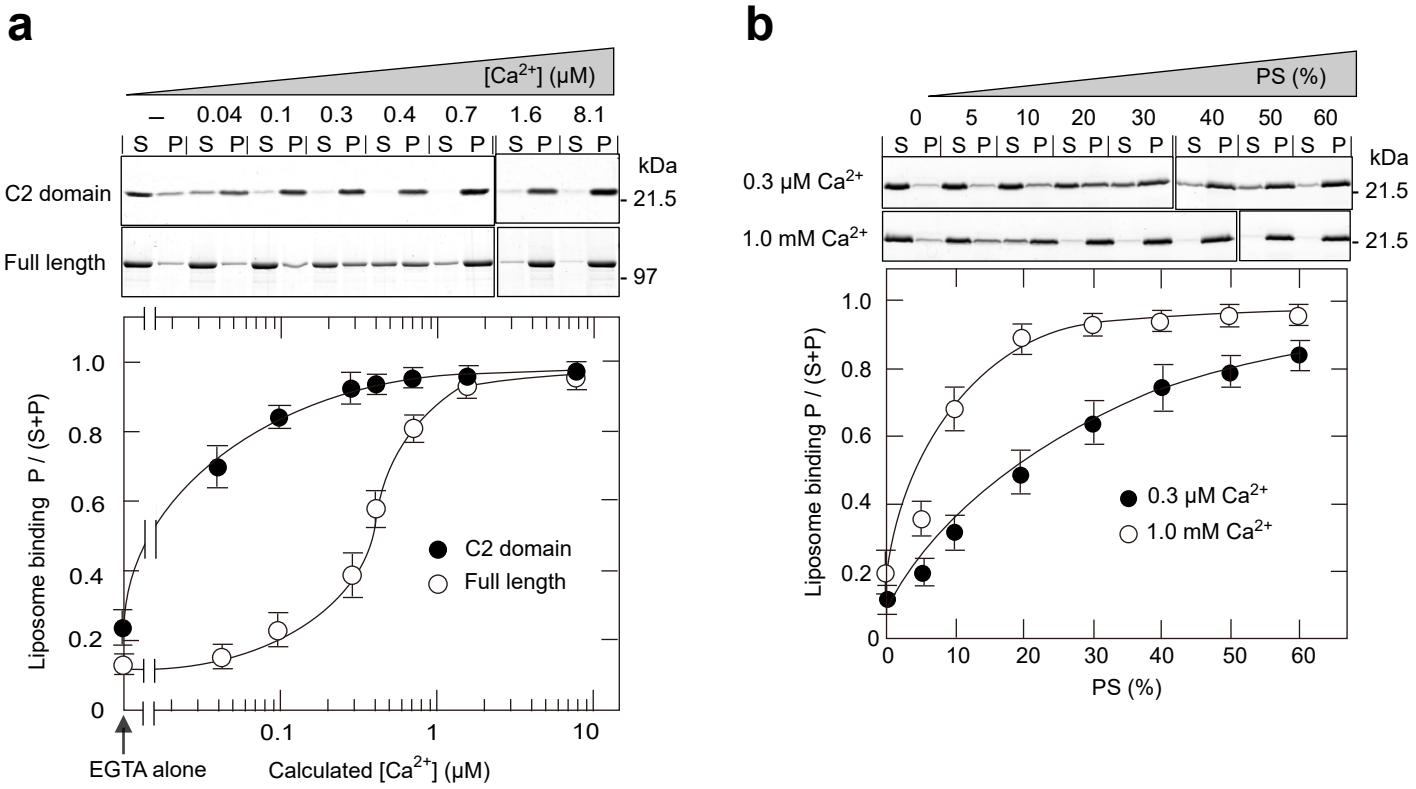

Extended Data Fig. 6 | The Nedd4L C2 domain is a Ca^{2+}-dependent PS binding domain. A co-sedimentation assay was performed with (a) the C2 domain or full-length Nedd4L using Folch liposomes at various Ca^{2+} concentrations and with (b) the C2 domain using synthetic liposomes containing various percentages of PS at 0.3 μM or 1.0 mM Ca^{2+}. The supernatant (S) and pellet (P) were subjected to SDS-PAGE, followed by CBB staining (upper panels). Bottom panels, quantitative analysis. (−) for [Ca^{2+}] indicates EGTA alone.

Extendedd Data Fig. 7

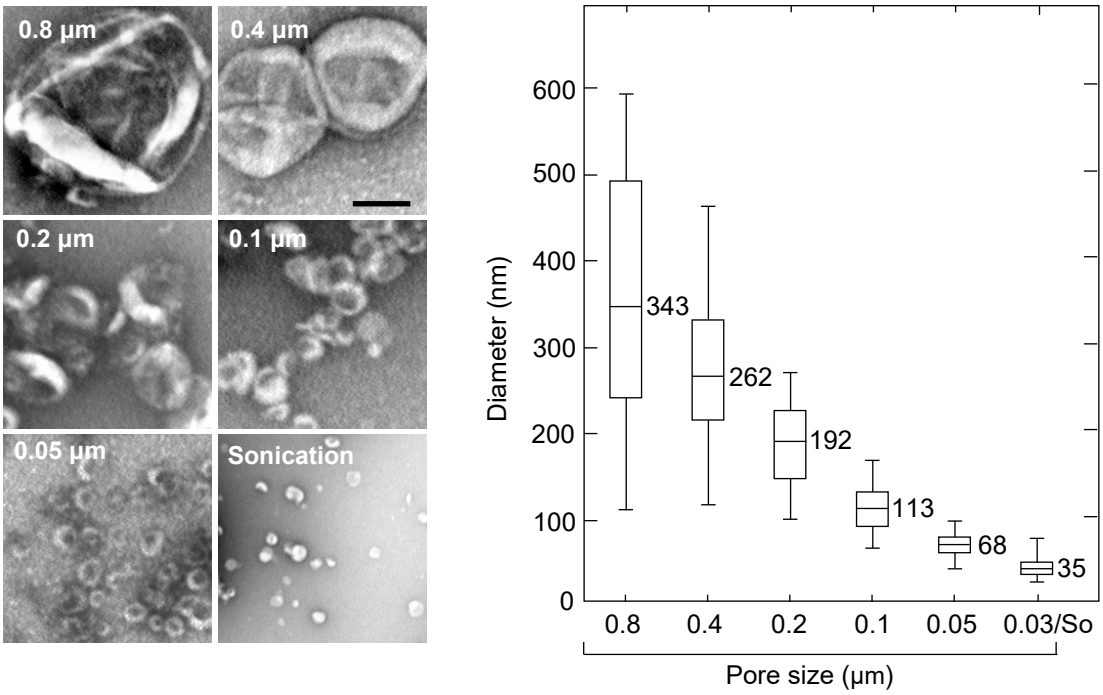

Extended Data Fig. 7 | Distribution of liposome diameters. Folch liposomes of different diameters were prepared by extrusion through the indicated pore sizes and sonication. Left panel, electron microscopic images. Scale bars, 200 nm. Right panel, quantitative analysis. So, sonication.

Extended Data Fig. 8

a

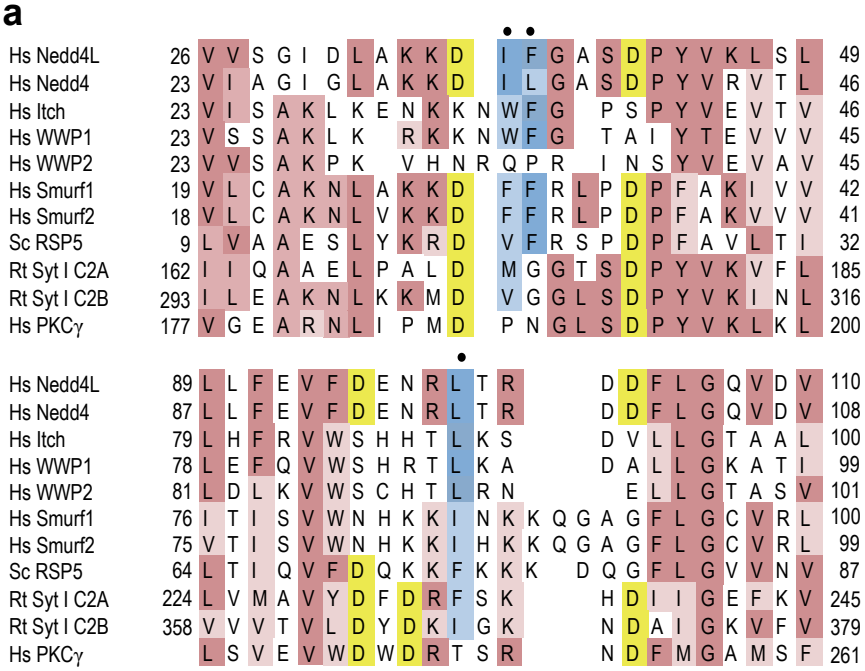

b

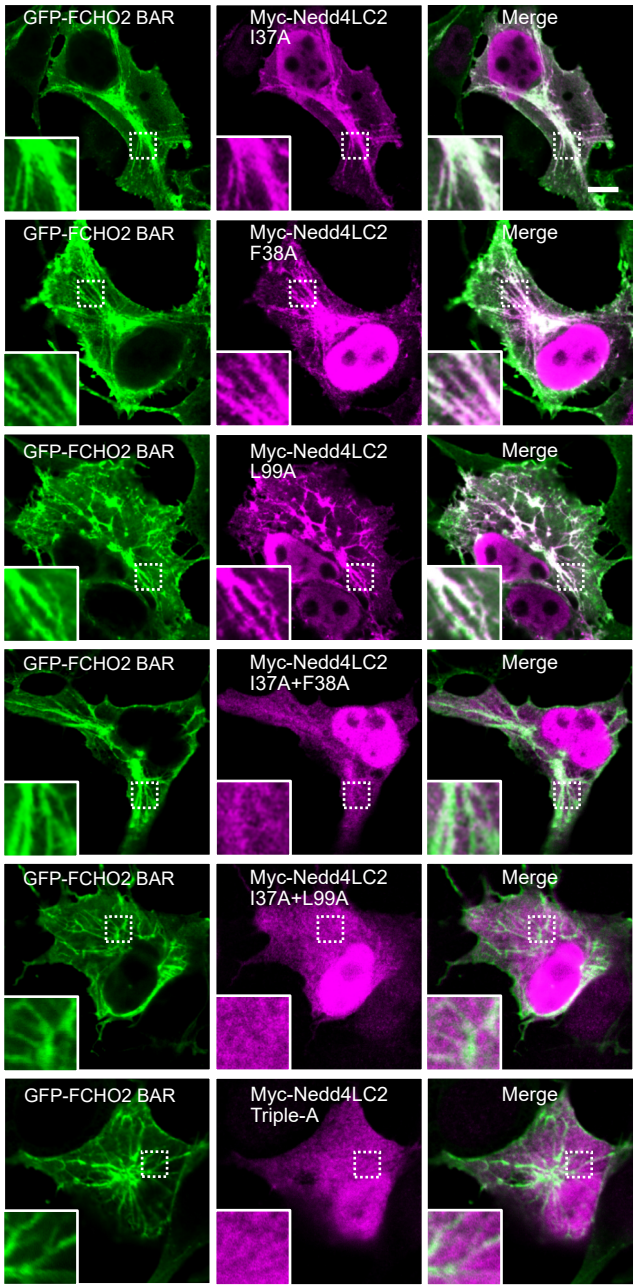

Extended Data Fig. 8 | Conserved hydrophobic residues of Nedd4L are responsible for sensing of membrane curvature. a, Sequence alignment of C2 domains. Conserved residues are highlighted with the following color code: yellow, aspartates for Ca^{2+} binding; blue, very hydrophobic residues probably for penetration into the lipid bilayer; and brown, others. Dots show the mutation sites. Hs, Homo sapiens; Sc, Saccharomyces cerevisiae; and Rt, Rattus norvegicus. **b,** Inability of Nedd4L C2 mutants to sense membrane curvature. GFP-FCHO2 BAR domain and Myc-Nedd4L C2 domain mutants were co-expressed in COS7 cells. Insets are enlarged images of dashed boxes. Scale bar, 10 μm.

Extended Data Fig. 9

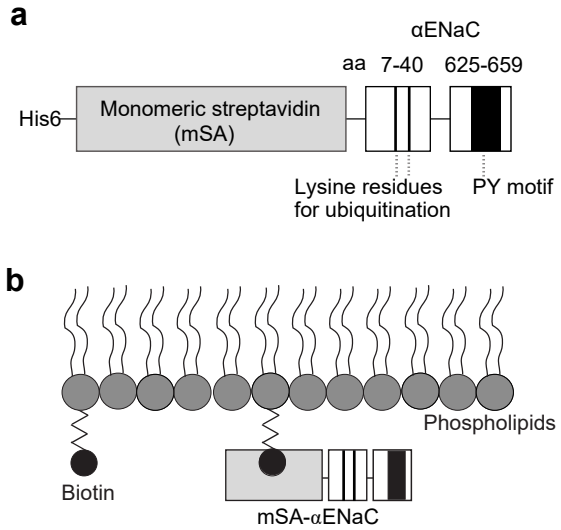

Extended Data Fig. 9 | Schematic diagrams of mSA-αENaC. a, Structure. **b**. Binding to biotinylated liposomes.

Extended Data Fig. 10

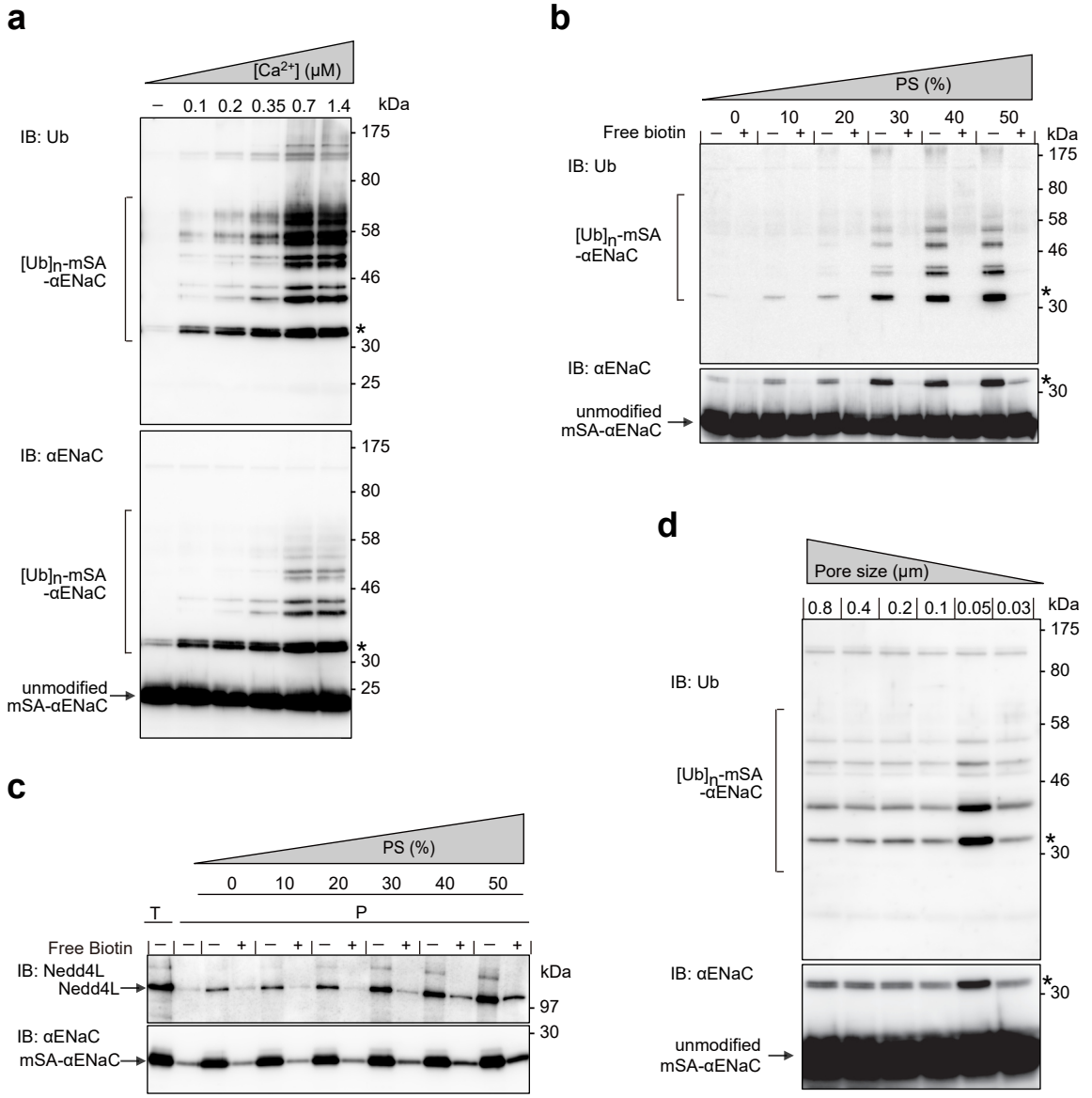

Extended Data Fig. 10 | Membrane binding and catalytic activity of Nedd4L. a–d, IB data of Fig. 4a, b, c, and d, respectively. Asterisks indicate the same band of mono-ubiquitinated mSA-αENaC.

Extended Data Fig. 11

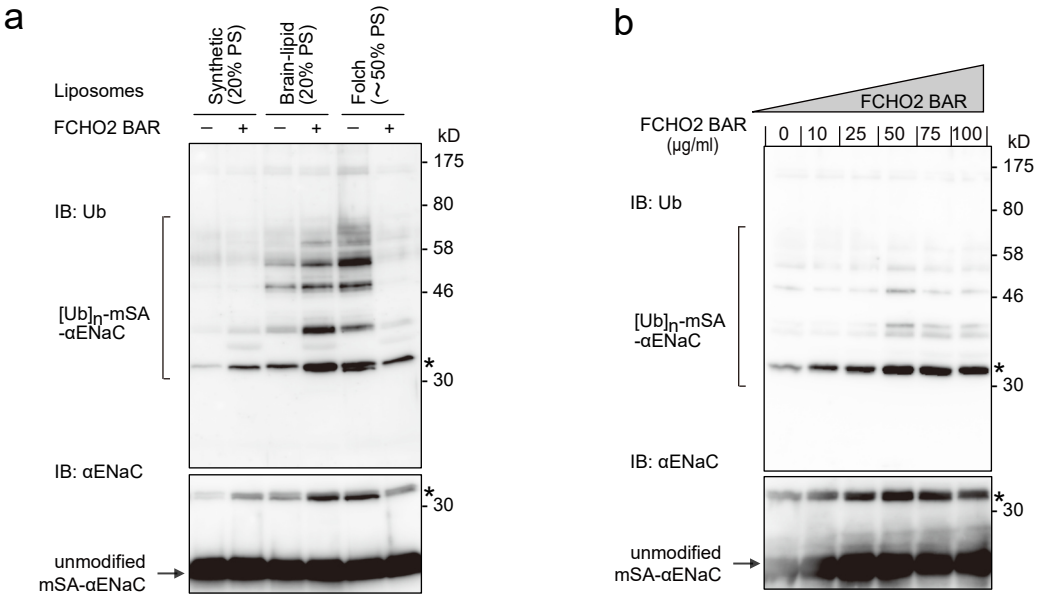

Extended Data Fig. 11 | FCHO2-induced activation of Nedd4L. a. Effects of various liposomes. A ubiquitination assay was performed with the FCHO2 BAR domain using synthetic (20% PS), brain-lipid (20% PS), or Folch liposomes (~50% PS). Samples were analyzed by IB. Asterisks indicate the same band of mono-ubiquitinated mSA-αENaC. **b**, Effects of various doses of the FCHO2 BAR domain. IB data of Fig. 4f.

Extended Data Fig. 12

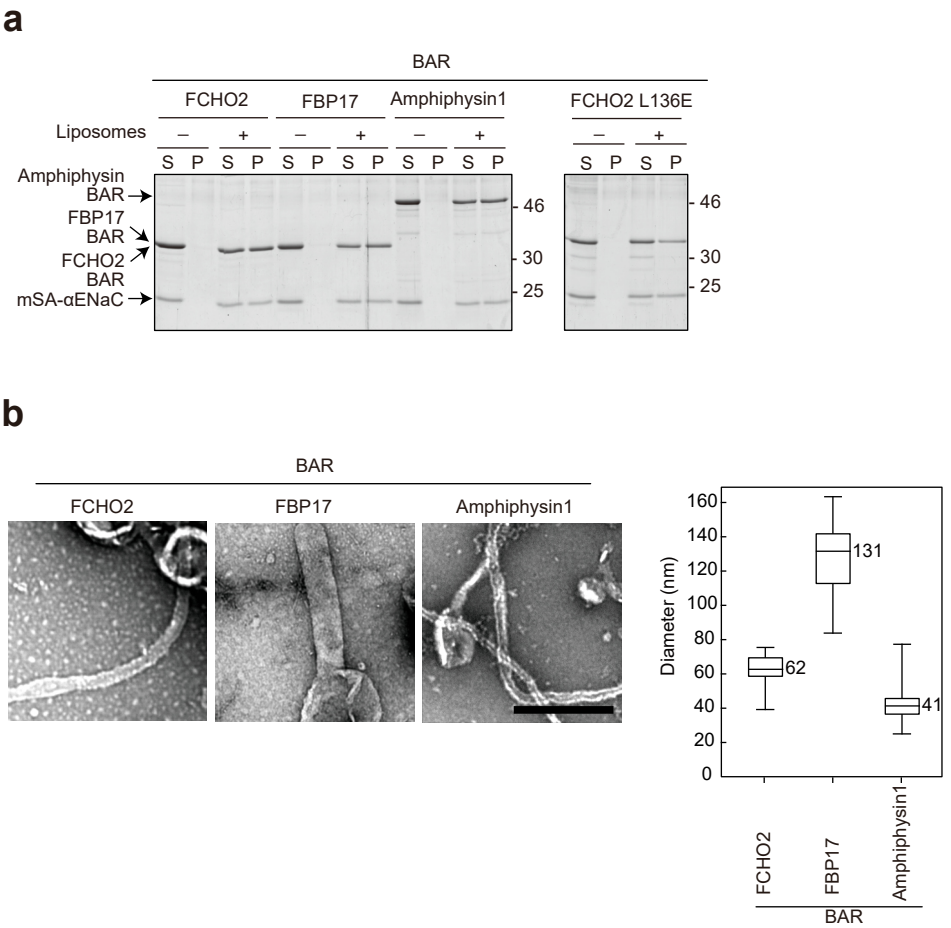

Extended Data Fig. 12 | Membrane binding and curvature generation of BAR domains and an FCHO2 mutant. Co-sedimentation (a) and *in vitro* tubulation (b) assays were performed at 0.7 μM Ca^{2+} with the indicated BAR domains using brain-lipid liposomes that were associated with mSA-αENaC. **a,** Membrane binding. The supernatant (S) and pellet (P) were subjected to SDS-PAGE followed by CBB staining. **b,** Curvature generation. Left panel, electron microscopic image. Scale bar, 200 nm. Right panel, distribution of tubule diameters.

Extended Data Fig. 13

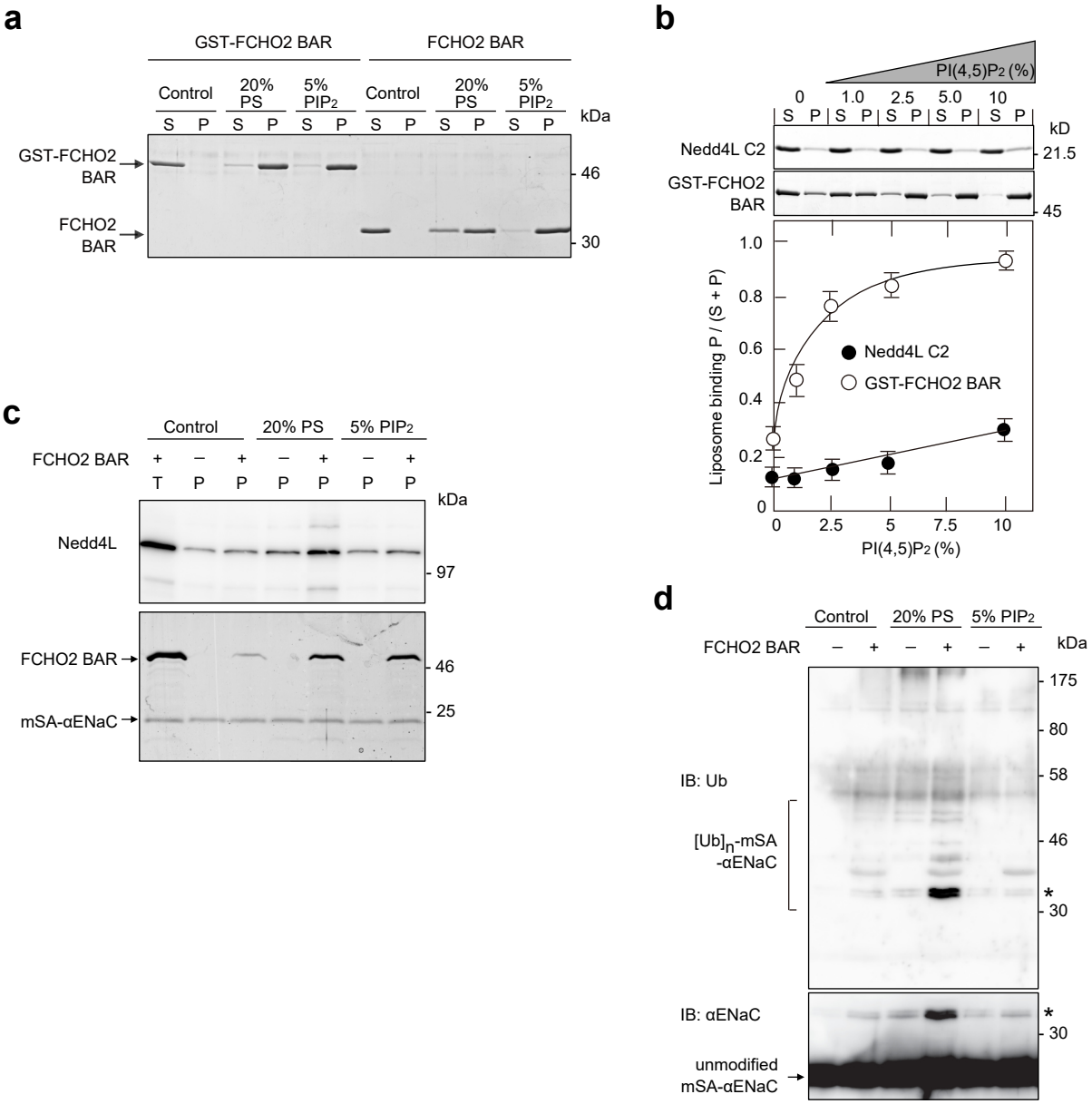

Extended Data Fig. 13 | Effects of PI(4,5)P_2 on FCHO2-induced recruitment and activation of Nedd4L. a, b, Binding to PI(4,5)P_2. A co-sedimentation assay was performed at 0.7 μM Ca^{2+} with the FCHO2 BAR or Nedd4L C2 domain using mSA-αENaC-associated synthetic liposomes containing (a) 20% PS, 5% PI(4,5)P_2, or (b) various percentages of PI(4,5)P_2. The supernatant (S) and pellet (P) were subjected to SDS-PAGE, followed by CBB staining. Bottom panel in b, quantitative analysis. Control, synthetic liposomes [0% PS and 0% PI(4,5)P2]. **c, d,** Effects on FCHO2-induced recruitment and activation of Nedd4L. Co-sedimentation (c) and ubiquitination (d) assays were performed at 0.7 μM Ca^{2+} with mSA-αENaC-associated synthetic liposomes containing 20% PS or 5% PI(4,5)P_2 in the presence or absence of the FCHO2 BAR domain. (c) Nedd4L recruitment. The total sample (T) and pellets (P) were subjected to SDS-PAGE, followed by IB with anti-Nedd4L antibody (upper panel) and CBB staining (lower panel). (d) Nedd4L activation. Samples were analyzed by IB. Asterisks indicate the same band of mono-ubiquitinated mSA-αENaC.

Extended Data Fig. 14

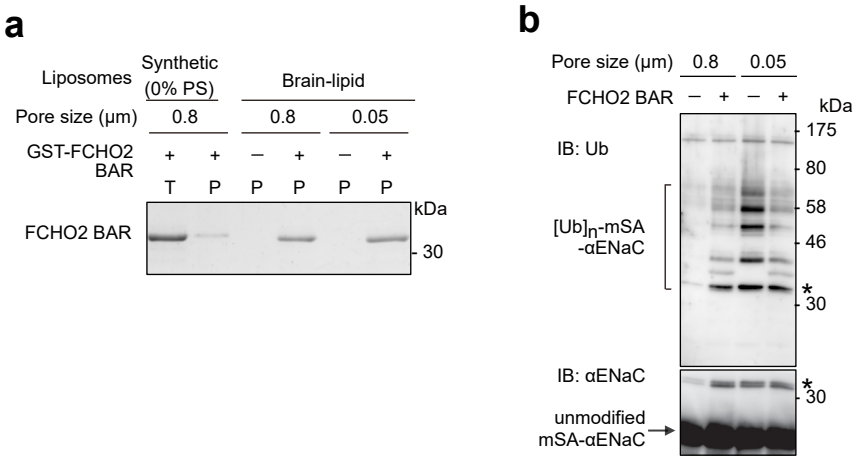

Extended Data Fig. 14 | Effects of liposome size on FCHO2-induced activation of Nedd4L. Co-sedimentation (a) and ubiquitination (b) assays were performed at 0.7 μM Ca^{2+} with the FCHO2 BAR domain using brain-lipid liposomes (0.8 μm or 0.05 μm pore-size) that were associated with mSA-αENaC. **a**, Binding of the FCHO2 BAR domain to 0.8 μm and 0.05 μm pore-size liposomes. The co-sedimentation assay with anti-fluorescein antibody was performed using synthetic (0% PS) or brain-lipid liposomes containing fluorescein-PE. The total sample (T) and pellets (P) were subjected to SDS-PAGE, followed by CBB staining. **b,** Effects of liposome size on FCHO2-induced activation of Nedd4L. Samples were analyzed by IB. Asterisks indicate the same band of mono-ubiquitinated mSA-αENaC.

Extended Data Fig.15

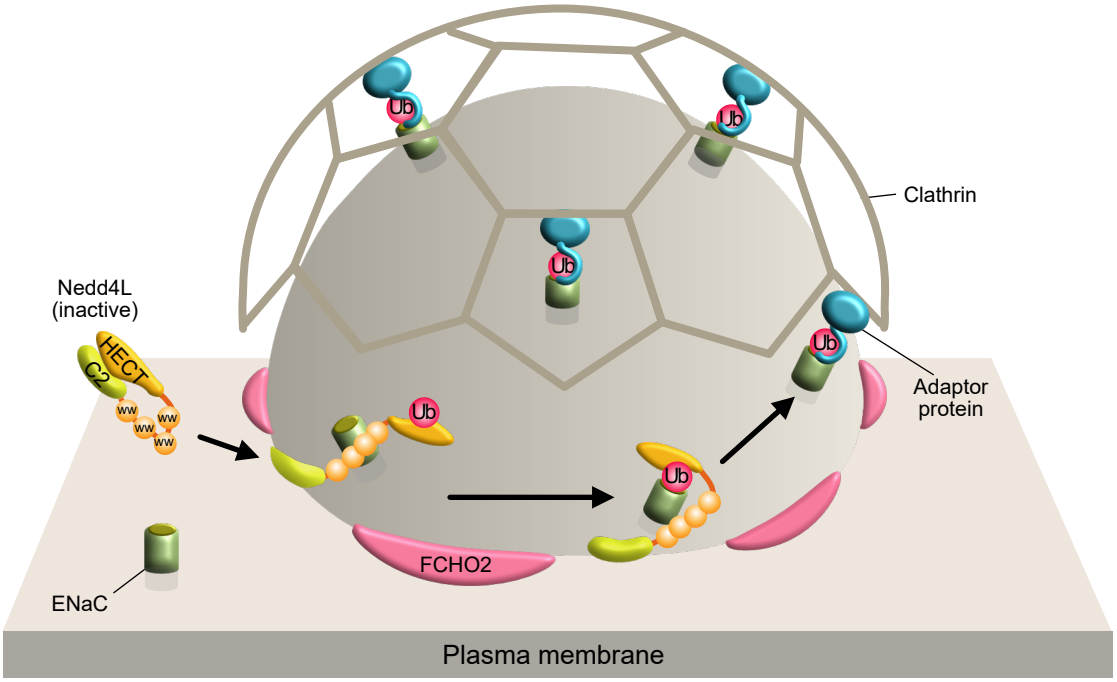

Extended Data Fig. 15 | Model of ENaC endocytosis.
FCHO2 binds to the plasma membrane and generates a specific degree of membrane curvature according to the intrinsic curvature of its BAR domain. Nedd4L exists in a catalytically autoinhibited state due to an intramolecular interaction between the N-terminal C2 and C-terminal HECT domains. Nedd4L is recruited to FCHO2-generated membrane curvature at the rim of nascent CCPs that ENaC enters. Membrane binding of the C2 domain causes catalytic activation by relieving autoinhibition. ENaC is ubiquitinated and captured by adaptor proteins with Ub-interacting motifs, such as Eps15.